NASA TN D-929

IN-02
386 502

TECHNICAL NOTE

D-929

EFFECTS AT MACH NUMBERS OF 1.61 AND 2.01 OF CAMBER AND TWIST ON THE AERODYNAMIC CHARACTERISTICS OF THREE SWEPT WINGS HAVING THE SAME PLANFORM

By Emma Jean Landrum and K. R. Czarnecki

Langley Research Center
Langley Field, Va.

NATIONAL AERONAUTICS AND SPACE ADMINISTRATION
WASHINGTON

August 1961

NATIONAL AERONAUTICS AND SPACE ADMINISTRATION

TECHNICAL NOTE D-929

EFFECTS AT MACH NUMBERS OF 1.61 AND 2.01 OF CAMBER AND TWIST ON THE AERODYNAMIC CHARACTERISTICS OF THREE SWEPT WINGS HAVING THE SAME PLANFORM

By Emma Jean Landrum and K. R. Czarnecki

SUMMARY

An investigation has been made at Mach numbers of 1.61 and 2.01 to determine the aerodynamic characteristics of three wings having a sweepback of 50° at the quarter-chord line, a taper ratio of 0.20, an NACA 65A005 thickness distribution, and an aspect ratio of 3.5. One wing was flat, one had at each spanwise station an a = 0 mean line modified to have a maximum height of 4-percent chord, and one had a linear variation of twist with 6° of washout at the tip. Tests were made with natural and fixed transition at Reynolds numbers ranging from 1.2×10^6 to 3.6×10^6 through an angle-of-attack range of -20° to 20°.

When compared with the flat wing, the effect of the linear variation of twist with 6° of washout at the tip was to increase the lift-drag ratio when the leading edge was subsonic; but little increase in lift-drag ratio was obtained when the leading edge was supersonic. Pitching moment was increased and gave a positive trim point without greatly affecting the rate of change of pitching moment with lift coefficient.

For the cambered wing the high minimum drag resulted in comparatively low lift-drag ratios. In addition, the pitching moments were decreased so that a negative trim point was obtained.

INTRODUCTION

The usefulness of camber and twist in the design of efficient wings for supersonic aircraft has been given considerable study over the past several years. Of current interest is the prediction of the changes in aerodynamic characteristics of wings when they distort under variable flight loads. In order to obtain some insight into these problems of distortion, a general investigation of the effects

of arbitrary camber and twist built into nearly rigid models is being made at low supersonic speeds by means of pressure-distribution and force tests. The tabulated results of a pressure investigation of the separate effects of camber and twist on the aerodynamic characteristics of a sweptback wing at Mach numbers of 1.61 and 2.01 are presented in reference 1, and a limited analysis of some of these results is presented in reference 2. The results of a force study of the same wings are presented herein.

The force tests were made on a basic semispan wing planform having a sweepback of 50° at the quarter-chord line, a taper ratio of 0.20, an NACA 65A005 thickness distribution, and an aspect ratio of 3.5. Three wings were tested: a flat wing, a wing having at each spanwise station an a = 0 mean line modified to have a maximum height of 4-percent chord, and a wing having a linear variation of twist with 6° of washout at the tip. Tests were made at Mach numbers of 1.61 and 2.01 over an angle-of-attack range from -20° to 20°. Tests were made with natural and fixed transition at Reynolds numbers, based on the wing mean aerodynamic chord, ranging from 1.2×10^6 to 3.6×10^6. Only a limited analysis and comparison with theory is presented.

SYMBOLS

b	wing span of complete wing
c	local chord
$\bar{c}$	mean aerodynamic chord, 10.33 in.
C_D	drag coefficient, Drag/qS
C_L	lift coefficient, Lift/qS
C_m	pitching-moment coefficient, $\frac{\text{Pitching moment}}{qS\bar{c}}$, pitching moment measured about $0.5\bar{c}$
C_l	rolling-moment coefficient (based on semispan), $\frac{\text{Rolling moment}}{qS\frac{b}{2}}$, rolling moment measured about root chord
L/D	lift-drag ratio
M	free-stream Mach number

q	free-stream dynamic pressure
R	Reynolds number based on $\bar{c}$
S	semispan wing area
α	angle of attack, deg

MODELS AND MODEL MOUNTING

L
1
1
8
9

Three semispan wing models having the same planform but different surface shapes were tested. One was flat (designated wing F), one was cambered (designated wing C), and the third was twisted (designated wing 1). These designations correspond to those used in reference 1.

All of the wings had an NACA 65A005 thickness distribution in the streamwise direction, 50° of sweepback of the quarter-chord line, a taper ratio of 0.20, and an aspect ratio of 3.5. The ordinates for the NACA 65A005 thickness distribution are given in reference 3. The cambered wing had, in the streamwise direction, at each spanwise station an NACA a = 0 mean line modified to have a maximum height of 4-percent chord. (See page 93 of ref. 4 for unmodified mean line.) The twisted wing was derived from the flat wing by rotation about the leading edge of each spanwise station. Wing 1 had a linear spanwise variation of twist with 6° of washout at the tip. A plan view of the models tested is shown in figure 1.

The semispan wings were mounted horizontally in the tunnel from a turntable in a boundary-layer bypass plate which was located vertically in the test section about 10 inches from the tunnel wall.

TESTS AND TEST PROCEDURES

The tests were conducted in the Langley 4- by 4-foot supersonic pressure tunnel at Mach numbers of 1.61 and 2.01. At both Mach numbers all the wings were tested with fixed and free transition. Transition was fixed about 1/2 inch from the wing leading edge by grains of No. 60 carborundum.

A four-component strain-gage balance located in the turntable of the boundary-layer bypass plate was used to measure the forces and moments on the wings. Angle of attack was changed manually by rotating the turntable on which the models were mounted and was measured by a vernier scale outside the tunnel.

The angle-of-attack range was from -20° to 20° although the complete range was not obtained for all the wings at all test conditions.

Tunnel stagnation pressures of 8 and 15 pounds per square inch absolute were used on the wings to span the range of Reynolds numbers. Generally, the Reynolds numbers, based on $\bar{c}$, ranged from 1.7×10^6 to 3.6×10^6. In addition some data were obtained on wing C at a tunnel stagnation pressure of 6 pounds per square inch absolute corresponding to Reynolds numbers, based on $\bar{c}$, of 1.4×10^6 at $M = 1.61$ and 1.2×10^6 at $M = 2.01$.

Measurements of tip deflection made during the tests indicate a maximum in aeroelastic twist variation for all wings occurred near an angle of attack of 10°. At a stagnation pressure of 15 pounds per square inch absolute, the aeroelastic tip twist for all wings was about 1.5° of washout at this angle of attack of 10°. Lower angles of attack or lower stagnation pressures gave proportionately smaller values of aeroelastic tip twist. Inasmuch as the aeroelastic twist is the same for all the wings and therefore has no effect on the increments due to camber or twist, the angles of attack have not been corrected to account for the aeroelastic effects.

RESULTS AND DISCUSSION

The aerodynamic characteristics of the various wings are presented for a Mach number of 1.61 in figures 2 to 7 and for a Mach number of 2.01 in figures 8 to 13. Theoretical predictions for lift coefficient are included for the flat and twisted wings.

Linear theory was used to calculate the theoretical lift-curve slopes for the flat wing (part (a) of figures 2, 3, 8, and 9). Theoretical span loadings, obtained from references 5 and 6 for $M = 1.61$ and from reference 7 for $M = 2.01$, were used to determine the lift increment due to wing twist. The combination of the flat-wing lift and the lift increment due to twist gives the theoretical predictions for the twisted wing plotted in part (a) of figures 4, 5, 10, and 11.

Comparison of experimental data with theory for the flat and twisted wings shows for the subsonic leading edge ($M = 1.61$) that the experimental lift-curve slope at $\alpha = 0^\circ$ is higher than the theoretical curve slope (figs. 2 to 5). For the supersonic leading edge ($M = 2.01$), the experimental lift-curve slope is about the same or slightly lower than the theoretical (figs. 8 to 11).

For all the models, increasing Reynolds number or fixing transition had little or no effect on lift coefficient, pitching-moment coefficient, or rolling-moment coefficient (figs. 2 to 13). Generally, drag coefficient increased slightly with Reynolds number for both natural and fixed transition; a result indicating that fully turbulent flow had not developed over the wings.

In order to examine more closely the effects of camber and twist, the variations of C_L with α, C_m with C_L, C_D with C_L, and L/D with C_L are given at both Mach numbers at a Reynolds number of approximately 1.8×10^6 with fixed transition in figures 14, 15, 16, and 17, respectively.

As shown by figure 14 the effect of a linear twist at a given α is to decrease the lift with little change in lift-curve slope. This result tends to confirm the theoretical assumption that the lift for a twisted wing is a linear combination of a lift increment due to twist and the basic lift of the untwisted wing. Cambering the wing increased the lift at a given α, but the variation of C_L with α became slightly nonlinear.

The effect of wing twist is to increase the pitching-moment coefficient at a given C_L so as to provide a positive trim point with only a minor change in the slope of the curve for C_m plotted against C_L as shown in figure 15. Camber decreases the pitching moment at a given C_L so that a negative trim point is obtained, and also slightly increases the slope of the curve for C_m plotted against C_L.

Figure 16 shows that twisting the wing increased minimum drag slightly but at the same time decreased drag due to lift. Obviously, the cambered wing of this investigation has too high a minimum drag (probably because of leading-edge separation on the wing lower surface as a result of excessive camber) but the drag-due-to-lift characteristics are better for the cambered wing than those for the twisted wing. It is possible that a wing which is cambered to produce a more reasonable minimum drag may not show as favorable drag-due-to-lift characteristics. This result would be true if the favorable drag-due-to-lift characteristics of the wing of this investigation are due in part to a relieving effect brought about by the elimination of the initial leading-edge separation on the lower surface.

The curves for the variation of L/D with C_L (fig. 17) show for positive angles of attack that twisting the wing when the leading edge is subsonic ($M = 1.61$) produces relatively large increases in L/D, but little increase in L/D is obtained when the leading edge is supersonic ($M = 2.01$). At both Mach numbers the high minimum drag for the cambered wing contributes to the low values of L/D.

CONCLUSIONS

The lift, drag, pitching-moment, and rolling-moment characteristics were obtained at Mach numbers of 1.61 and 2.01 for three wings in order to examine the effect of twist and camber.

When compared with the flat wing, the effect of the linear variation of twist with 6° of washout at the tip was to increase the lift-drag ratio when the leading edge was subsonic (M = 1.61); but little increase in lift-drag ratio was obtained when the leading edge was supersonic (M = 2.01). Pitching-moment coefficient was increased and gave a positive trim point without greatly affecting the rate of change of pitching moment with lift coefficient.

For the cambered wing the high minimum drag resulted in comparatively low lift-drag ratios. In addition, the pitching moments were decreased so that a negative trim point was obtained.

Langley Research Center,
National Aeronautics and Space Administration,
Langley Field, Va., May 26, 1961.

REFERENCES

1. Grant, Frederick C.: A Tabulation of Wind-Tunnel Pressure Data at Mach Numbers of 1.61 and 2.01 for Five Swept Wings of the Same Plan Form but Different Surface Shapes. NACA RM L58D23, 1958.

2. Grant, Frederick C., and Mugler, John P., Jr.: Span Loadings Due to Wing Twist at Transonic and Supersonic Speeds. NACA RM L57D24a, 1957.

3. Patterson, Elizabeth W., and Braslow, Albert L.: Ordinates and Theoretical Pressure-Distribution Data for NACA 6- and 6A-Series Airfoil Sections With Thicknesses From 2 to 21 and From 2 to 15 Percent Chord, Respectively. NASA TR R-84, 1961. (Supersedes NACA TN 4322.)

4. Abbott, Ira H., Von Doenhoff, Albert E., and Stivers, Louis S., Jr.: Summary of Airfoil Data. NACA Rep. 824, 1945. (Supersedes NACA WR L-560.)

5. Heaslet, Max. A., and Lomax, Harvard: Supersonic and Transonic Small Perturbation Theory. General Theory of High Speed Aerodynamics. Vol. VI of High Speed Aerodynamics and Jet Propulsion, sec. D, ch. 3, W. R. Sears, ed., Princeton Univ. Press, 1954, pp. 186-206.

6. Lomax, Harvard, Heaslet, Max. A., and Fuller, Franklyn B.: Integrals and Integral Equations in Linearized Wing Theory. NACA Rep. 1054, 1951. (Supersedes NACA TN 2252.)

7. Kainer, Julian H.: Equations for the Loading on Triangular Wings Having Supersonic Leading and Trailing Edges Due to Various Basic Twist Distributions. Jour. Aero. Sci., vol. 20, no. 7, July 1953, pp. 469-476.

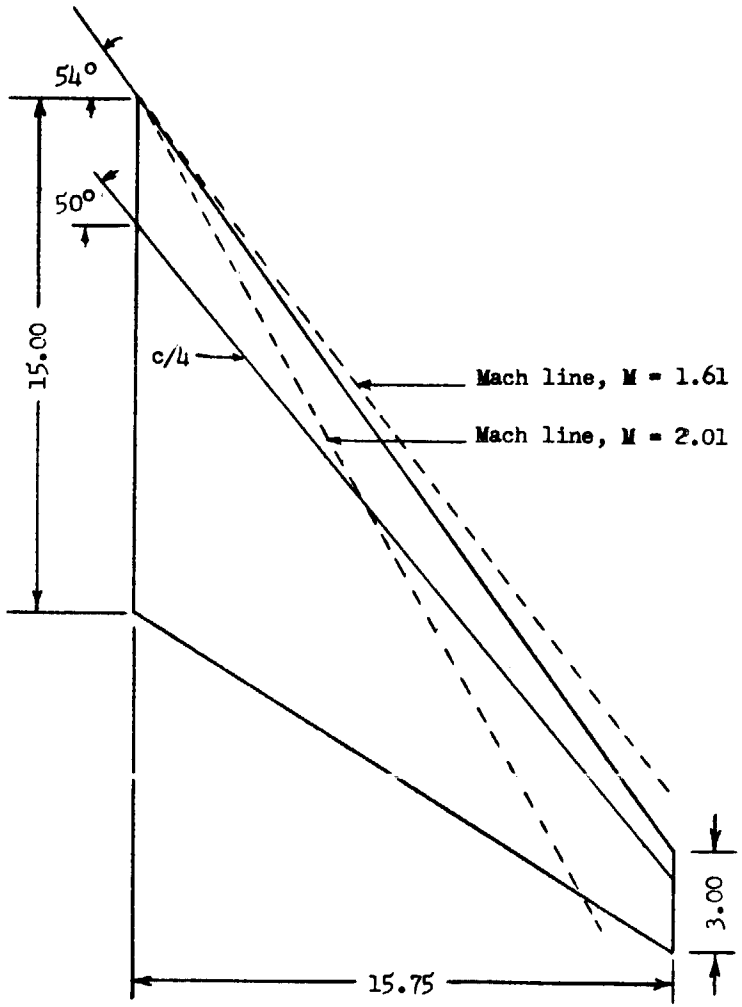

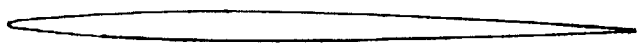

Root section
Flat and twisted wings

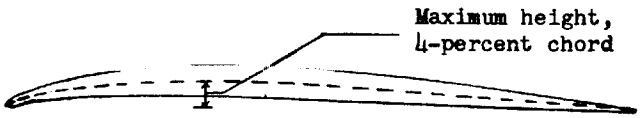

Root section
Cambered wing

Figure 1.- Planform and root sections of wings tested. (All dimensions are in inches. Sections not to planform scale.)

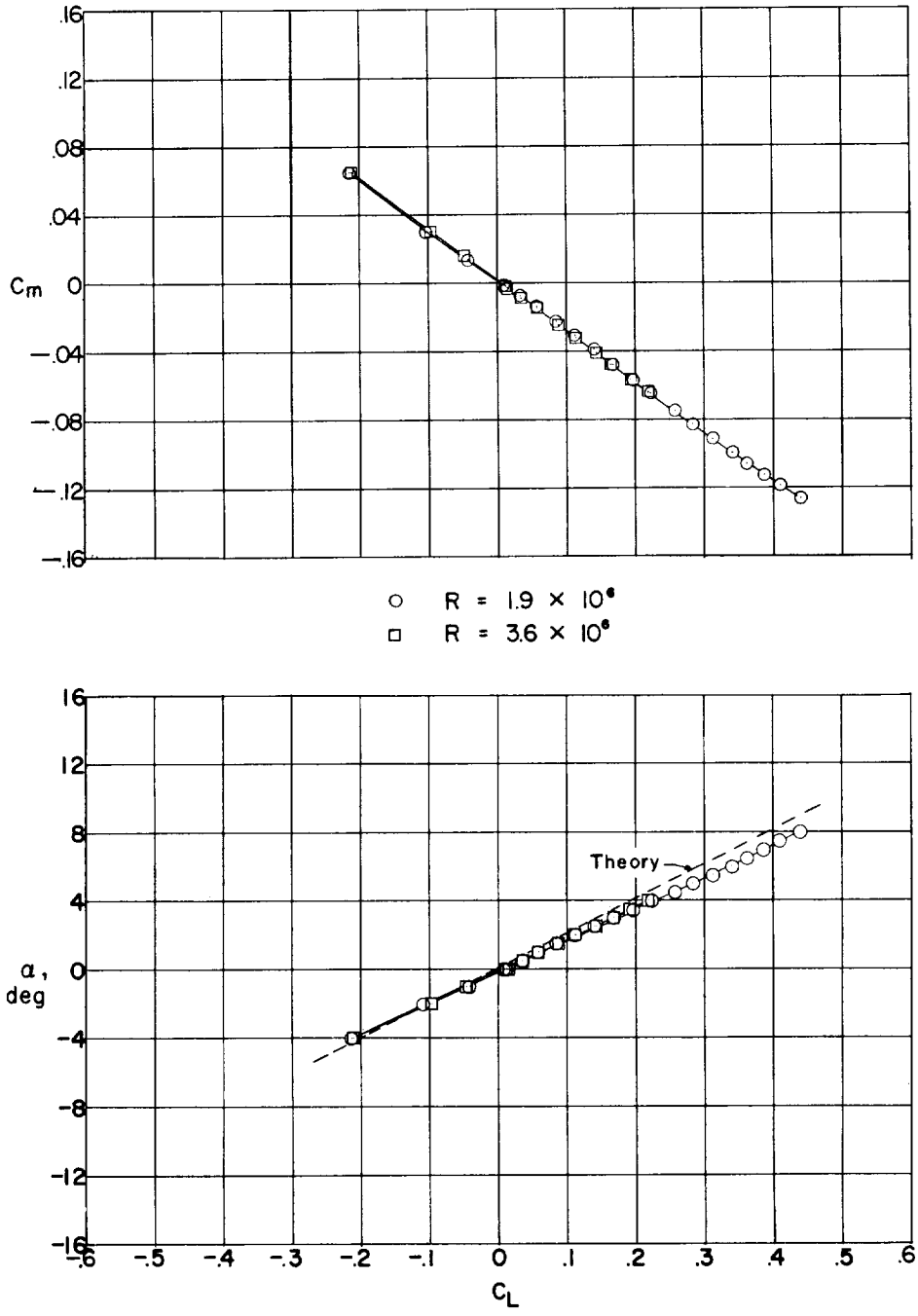

(a) Lift and pitching-moment coefficients.

Figure 2.- Aerodynamic characteristics of wing F with natural transition. M = 1.61.

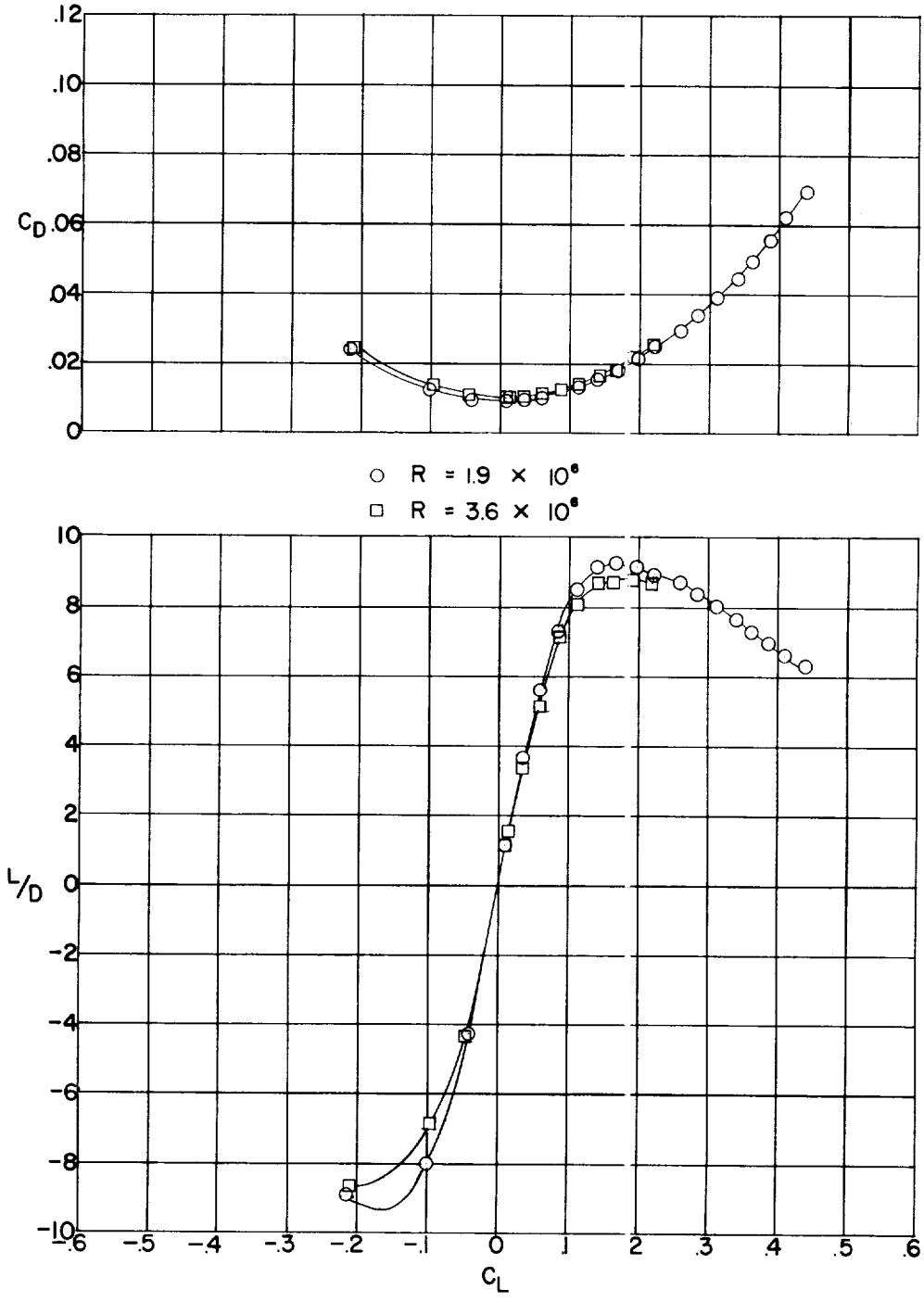

(b) Drag coefficient and lift-drag ratio.

Figure 2.- Continued.

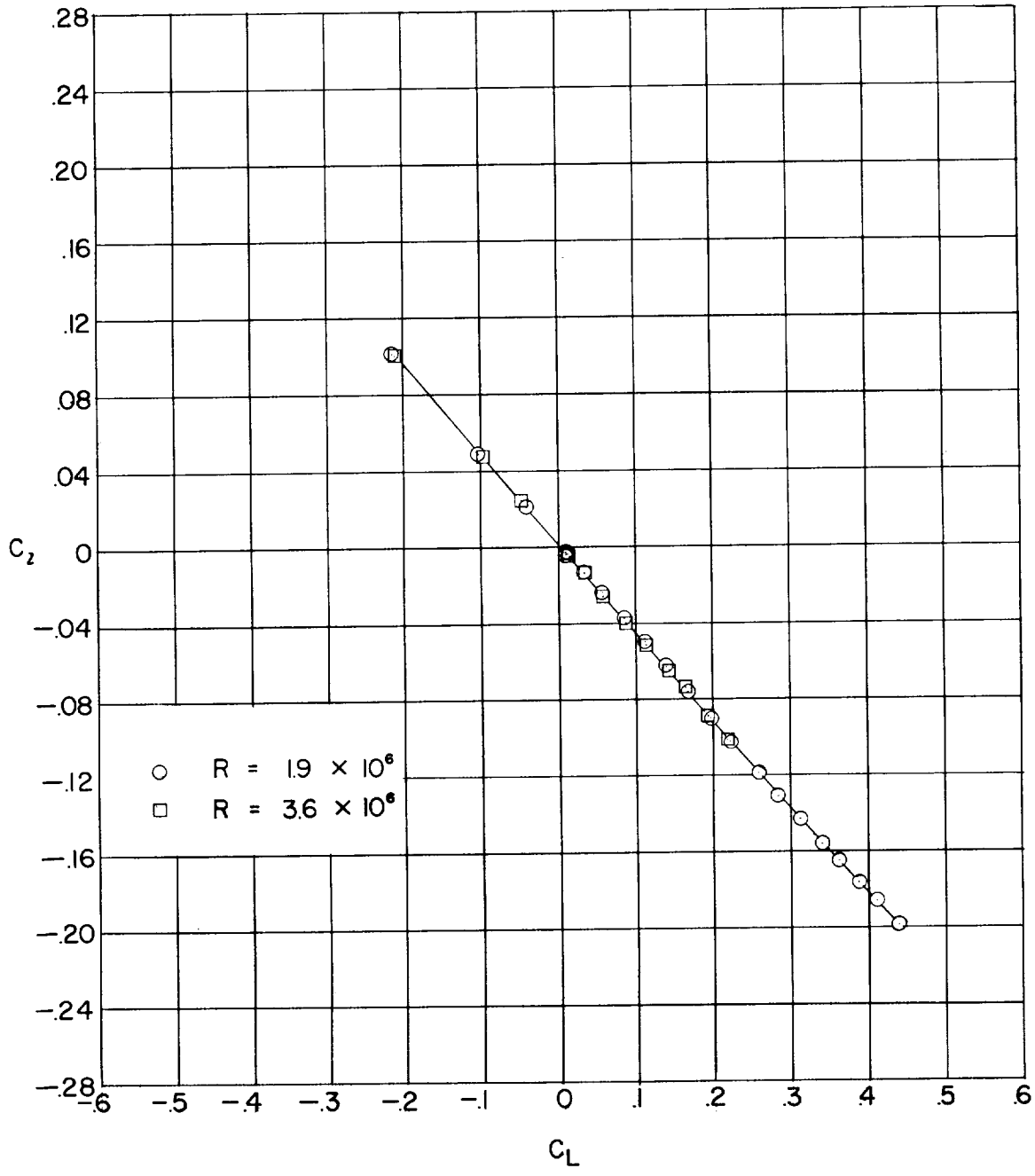

(c) Rolling-moment coefficient.

Figure 2.- Concluded.

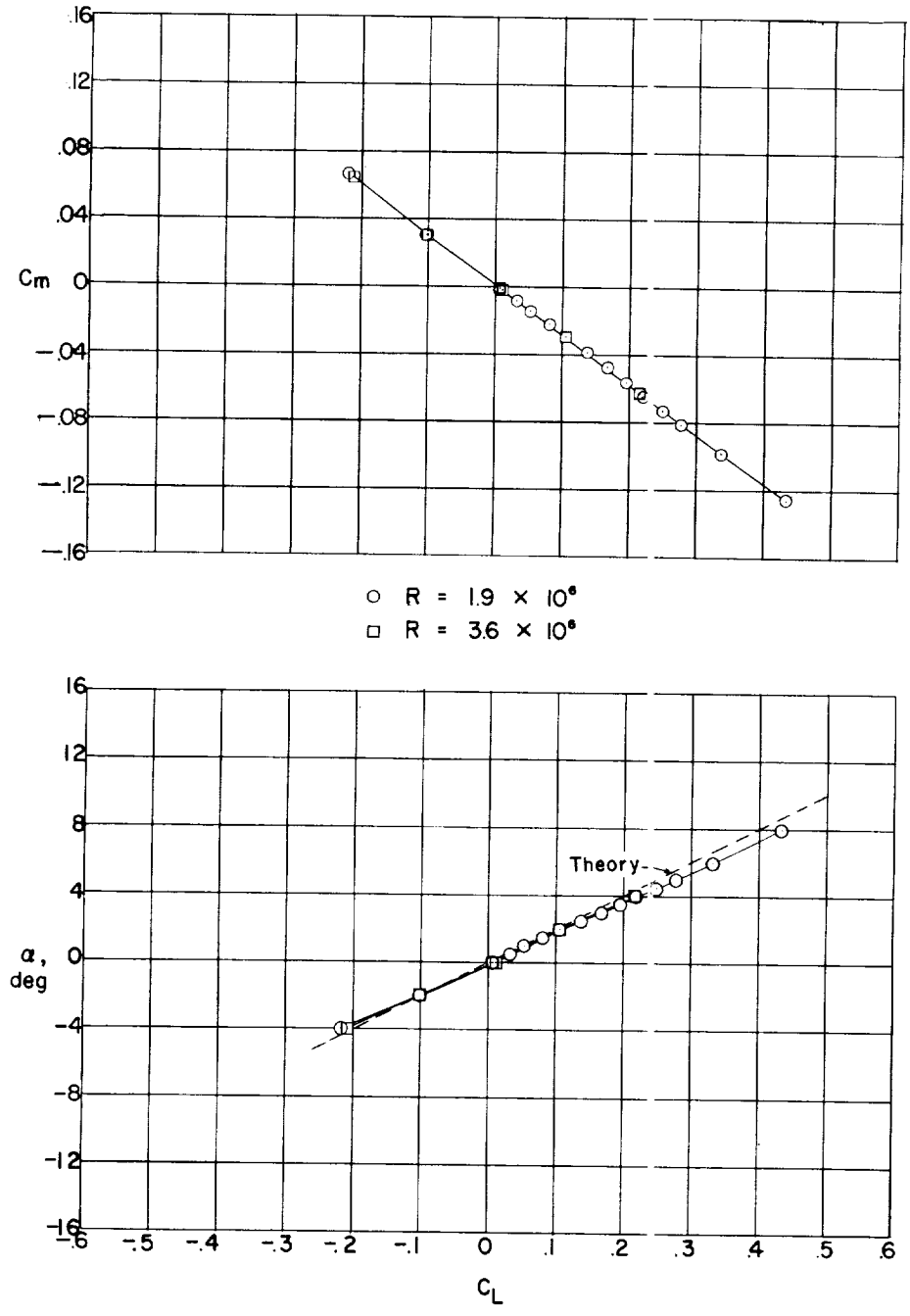

(a) Lift and pitching-moment coefficients.

Figure 3.- Aerodynamic characteristics of wing I' with fixed transition. M = 1.61.

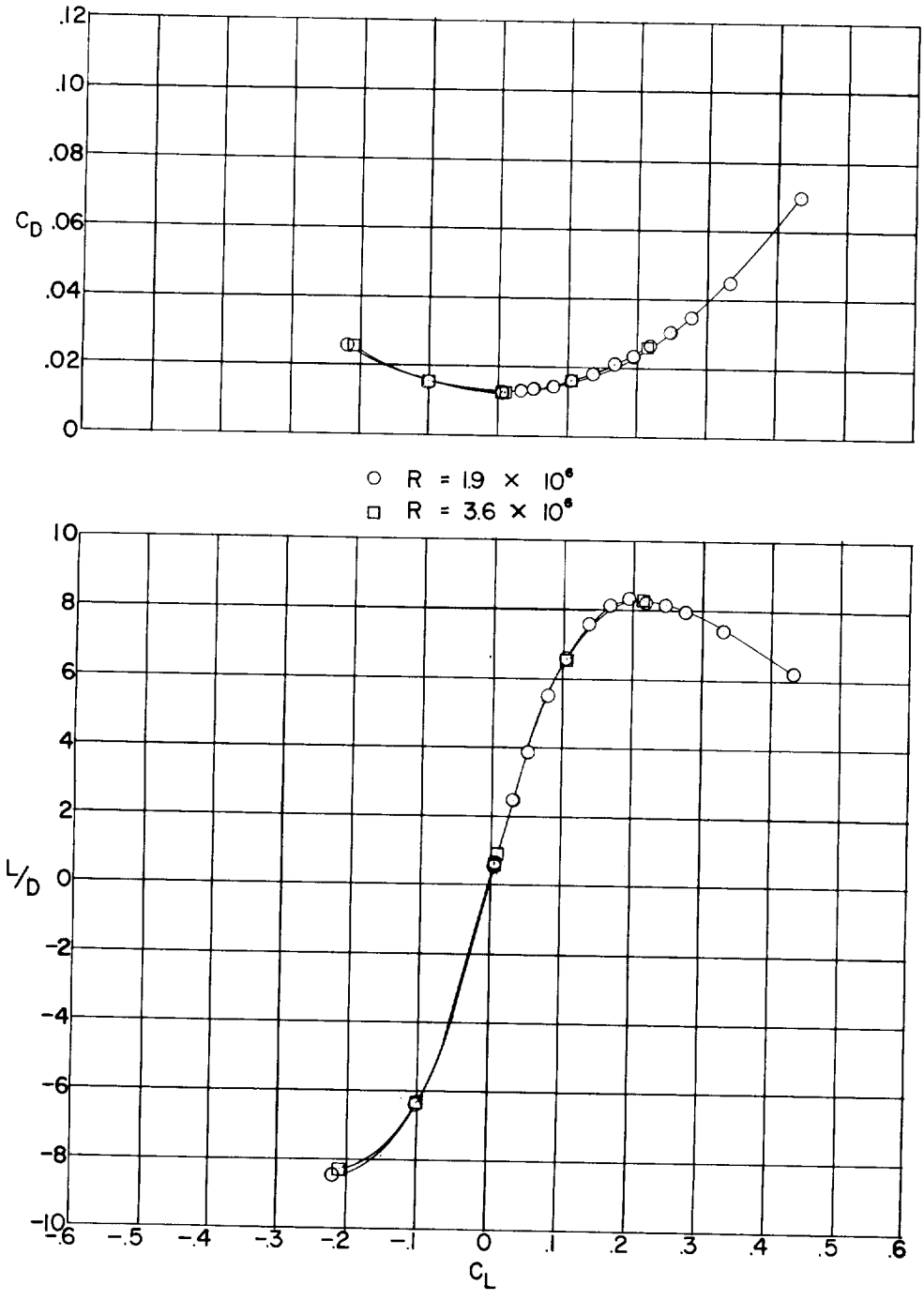

(b) Drag coefficient and lift-drag ratio.

Figure 3.- Continued.

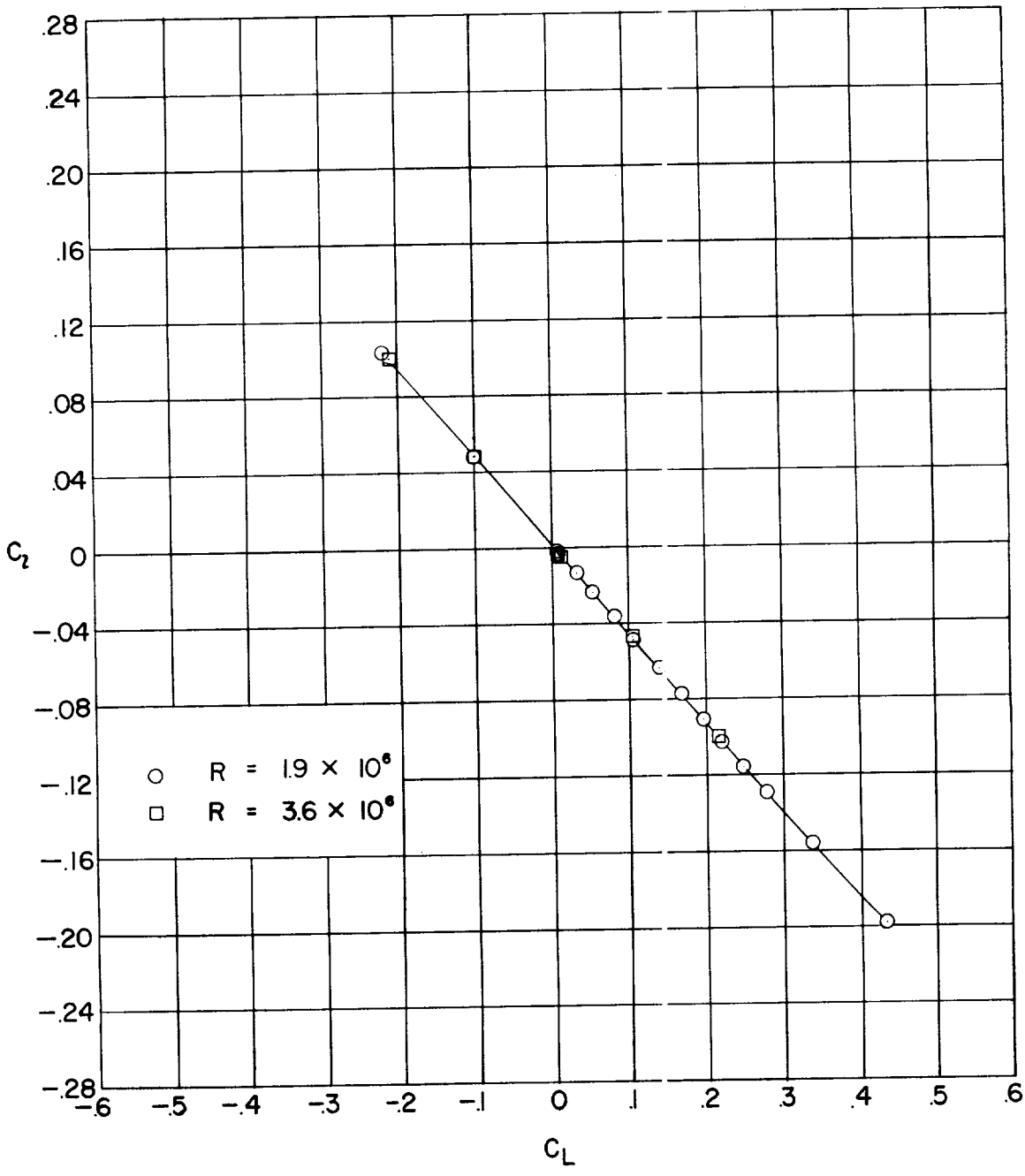

(c) Rolling-moment coefficient.

Figure 3.- Concluded.

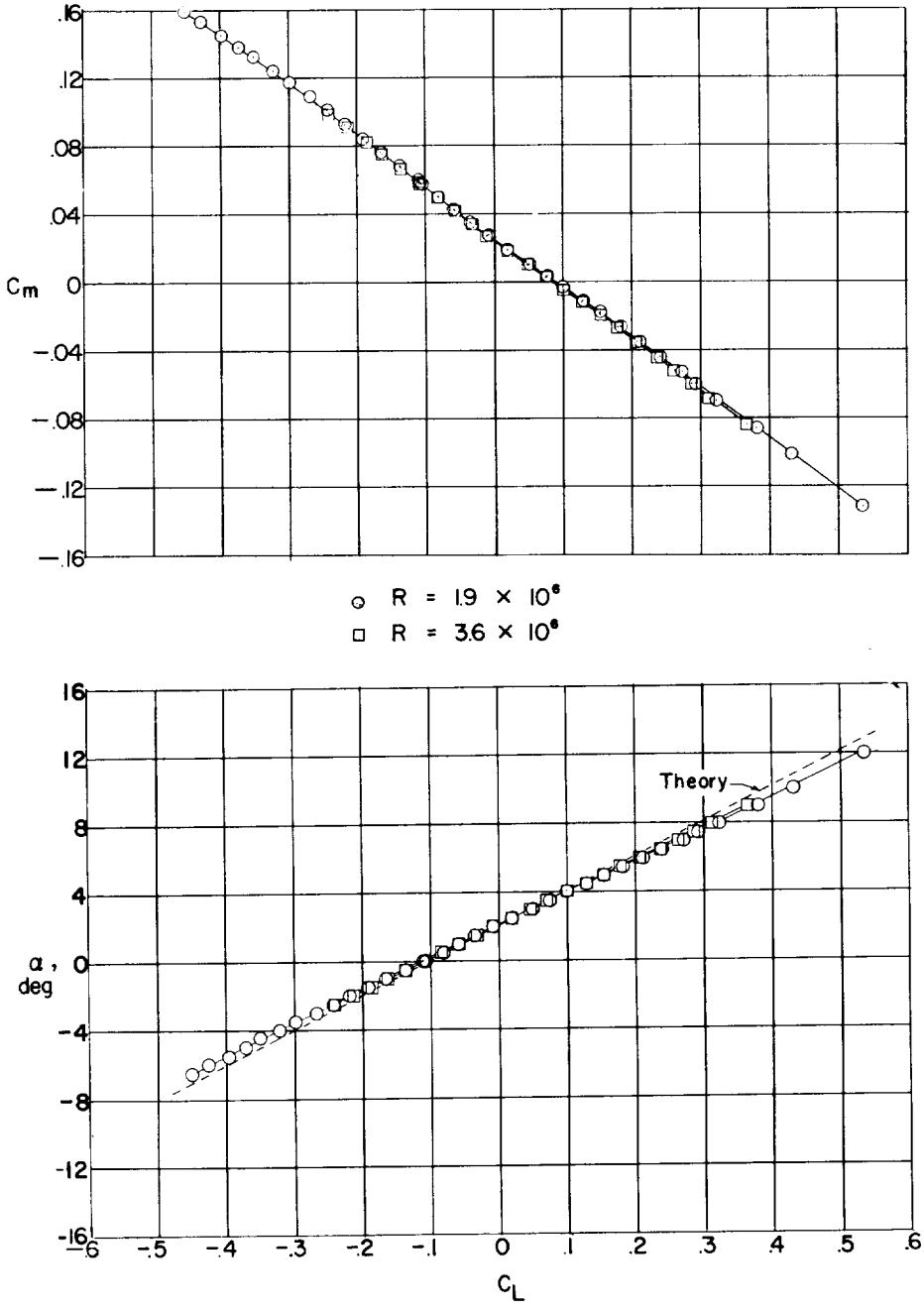

(a) Lift and pitching-moment coefficients.

Figure 4.- Aerodynamic characteristics of wing 1 with natural transition. M = 1.61.

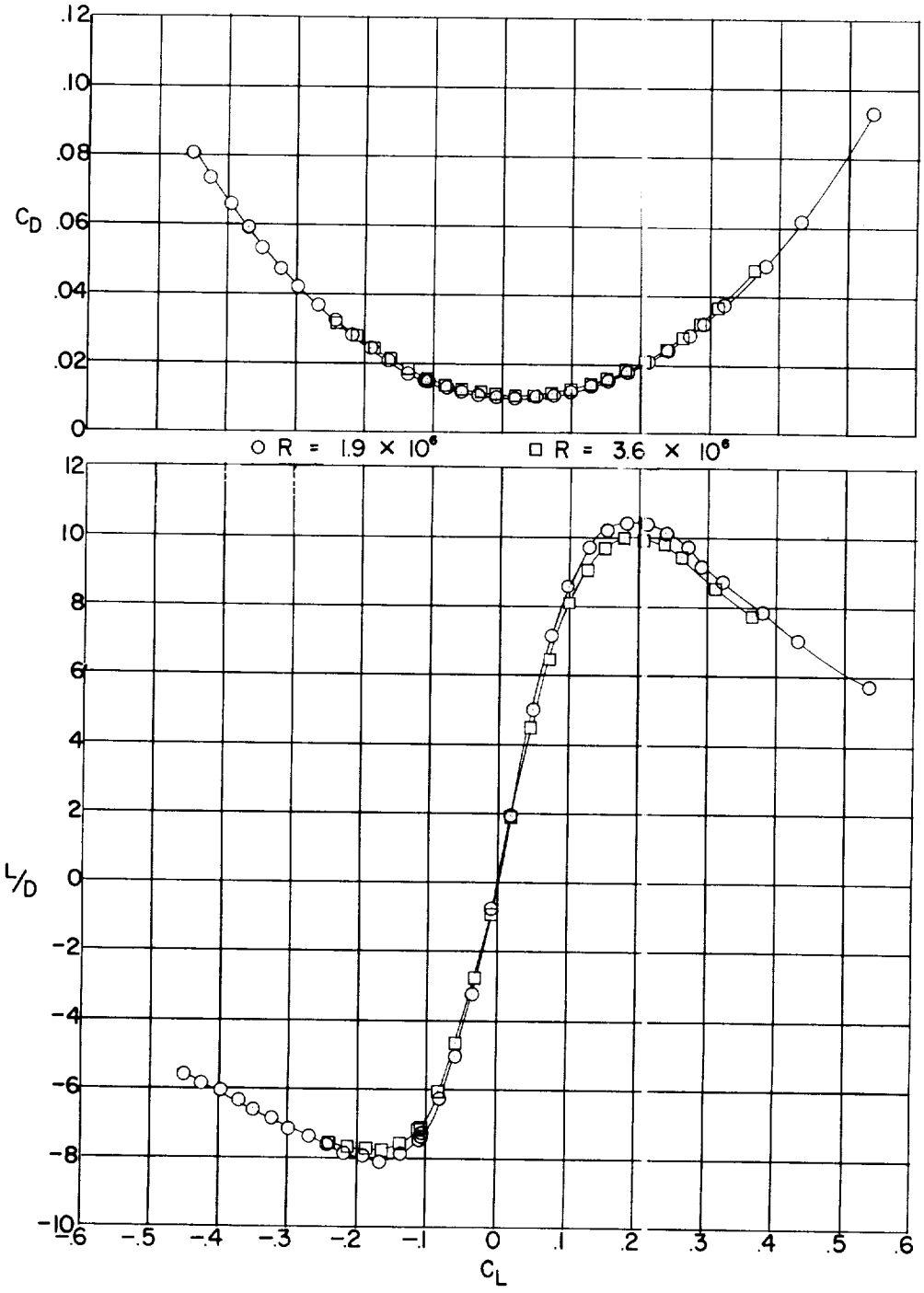

(b) Drag coefficient and lift-drag ratio.

Figure 4.- Continued.

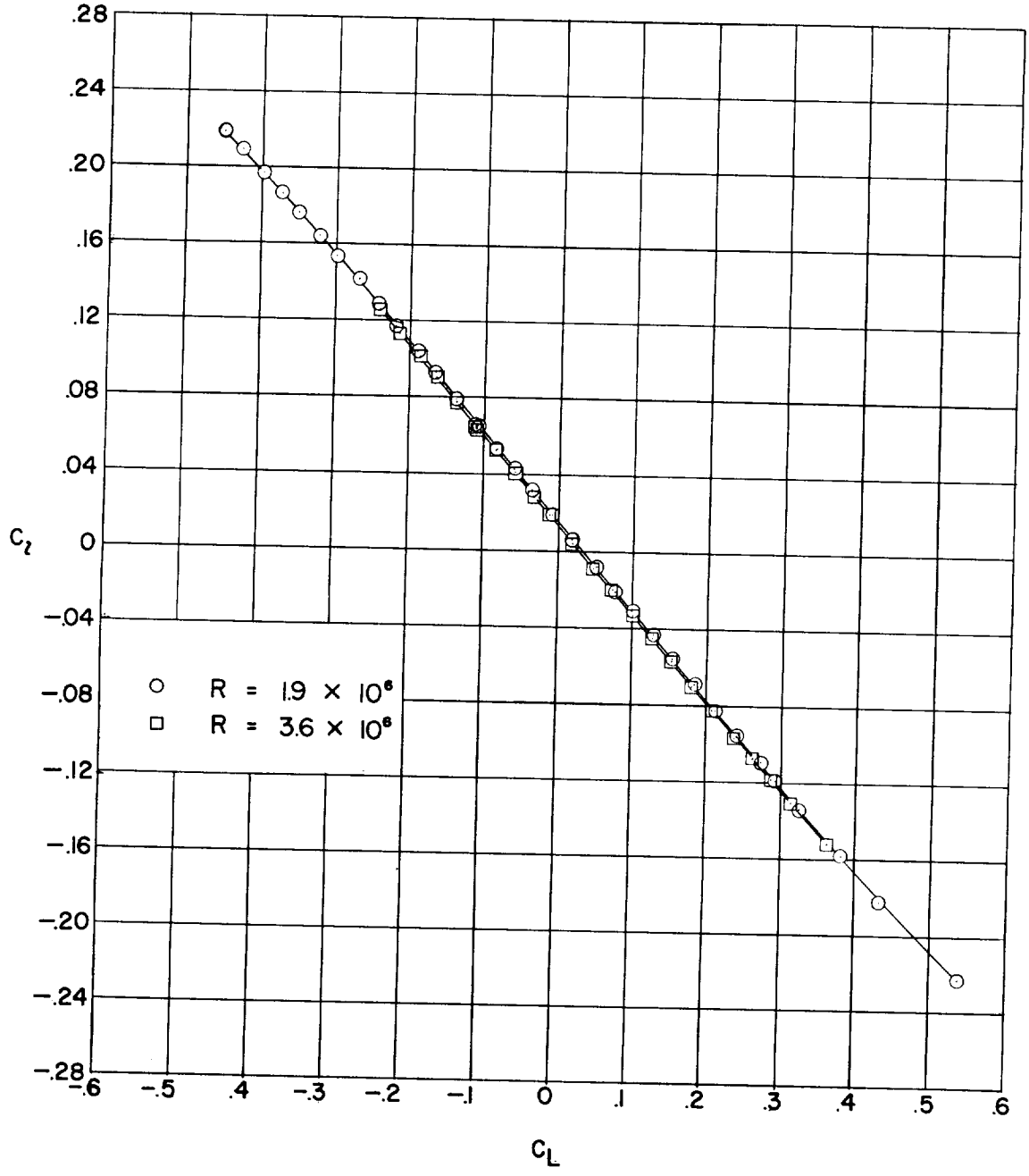

(c) Rolling-moment coefficient.

Figure 4.- Concluded.

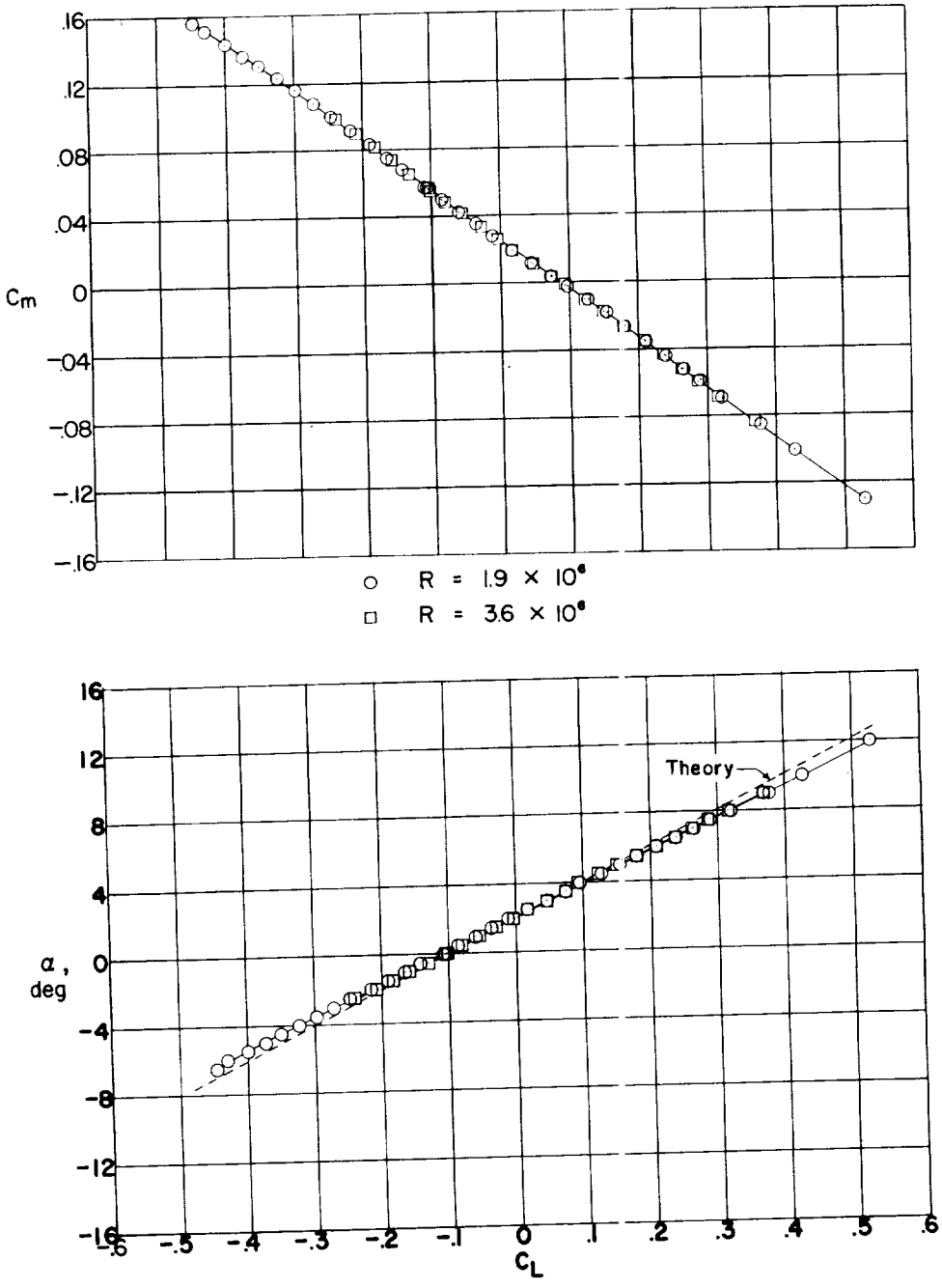

(a) Lift and pitching-moment coefficients.

Figure 5.- Aerodynamic characteristics of wing 1 with fixed transition. M = 1.61.

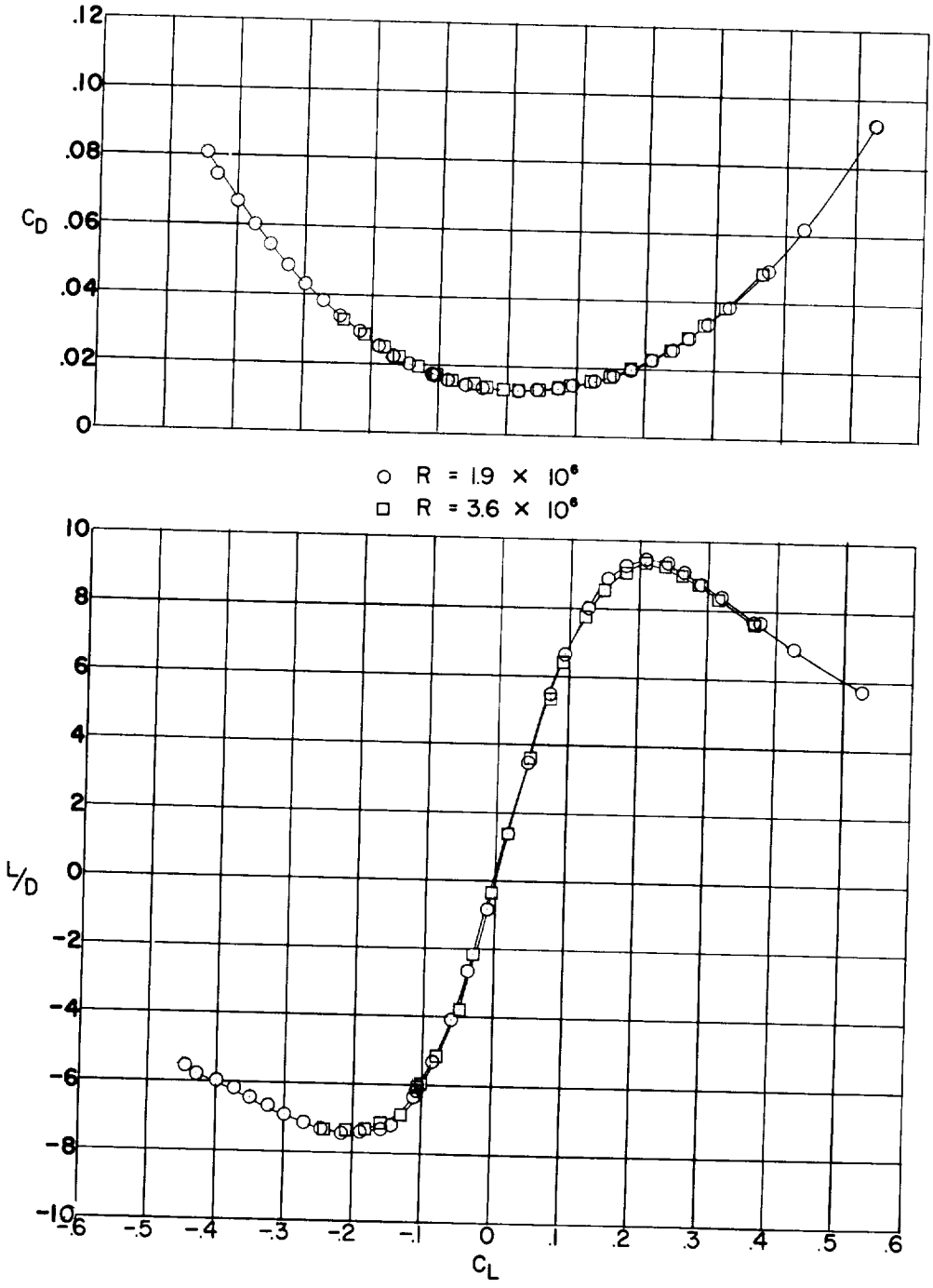

(b) Drag coefficient and lift-drag ratio.

Figure 5.- Continued.

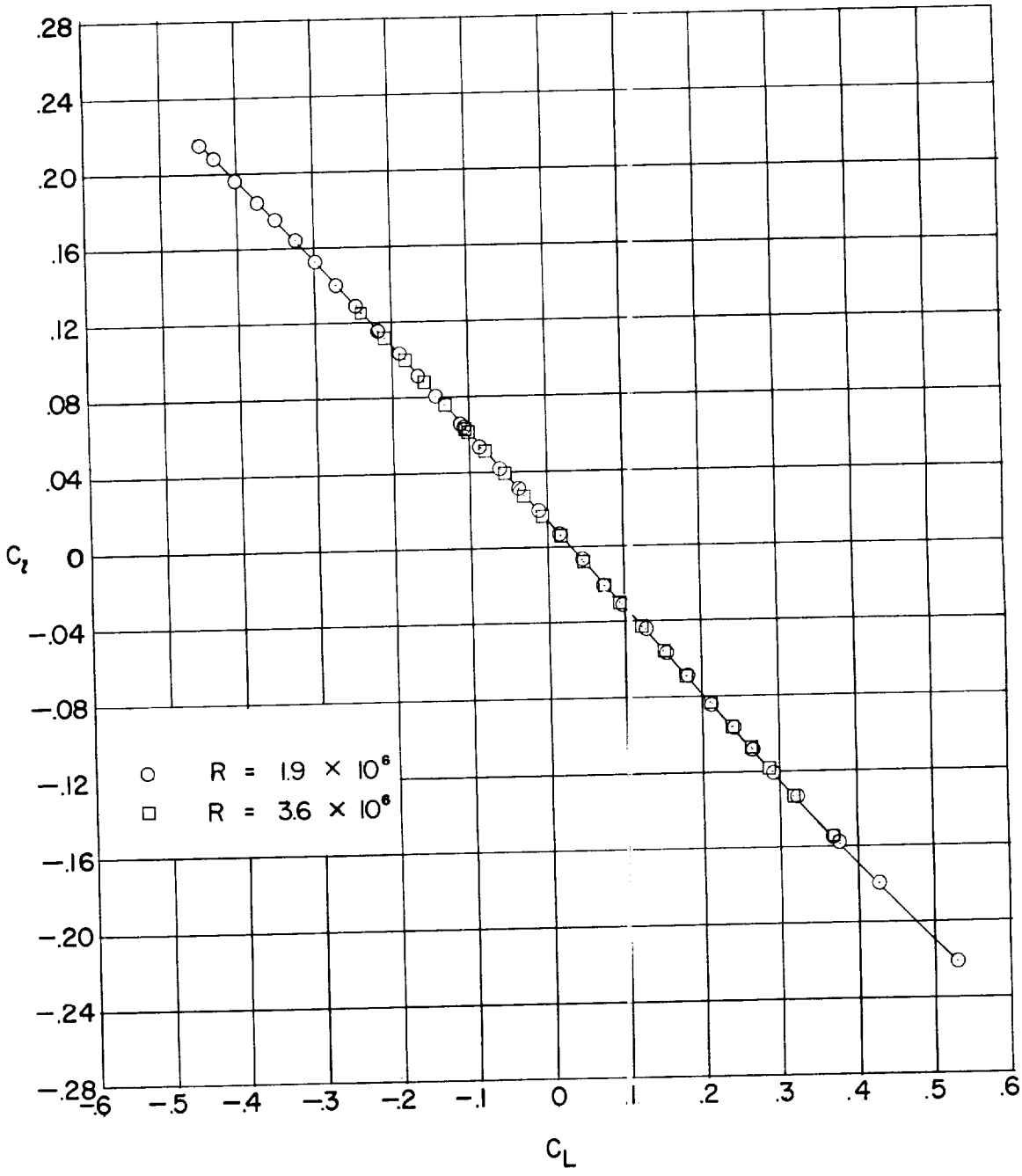

(c) Rolling-moment coefficient.

Figure 5.- Concluded.

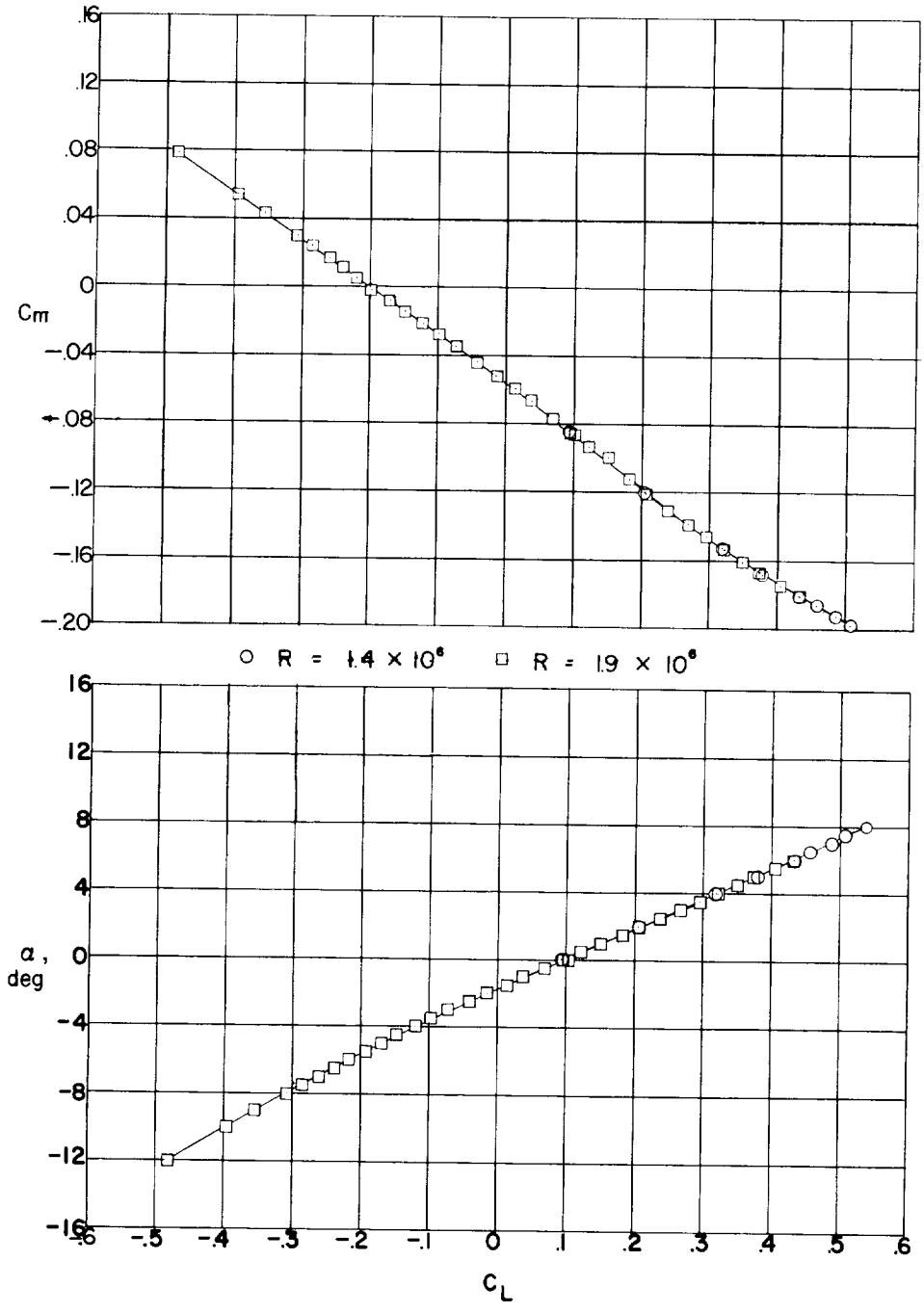

(a) Lift and pitching-moment coefficients.

Figure 6.- Aerodynamic characteristics of wing C with natural transition. M = 1.61.

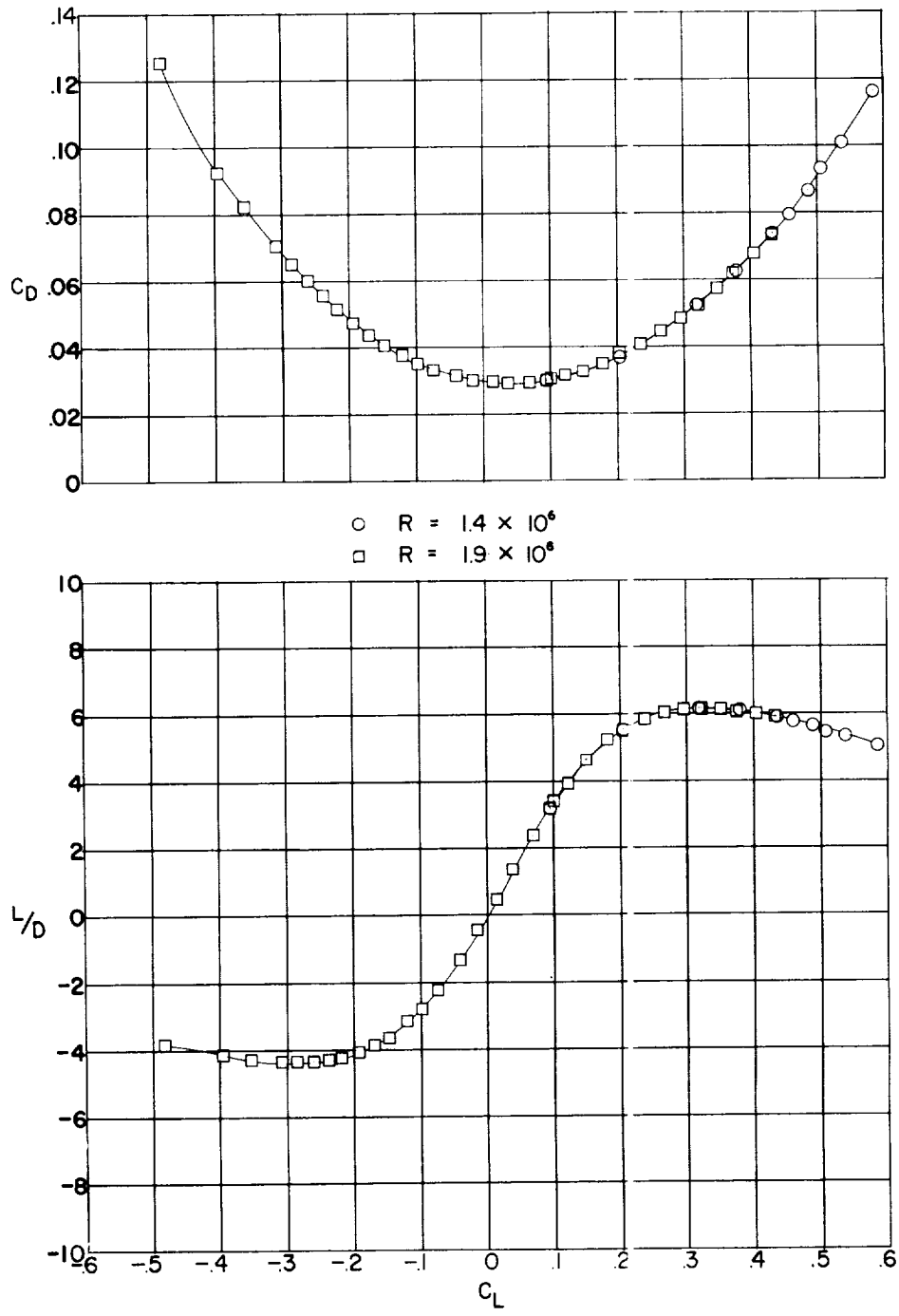

(b) Drag coefficient and lift-drag ratio.

Figure 6.- Continued.

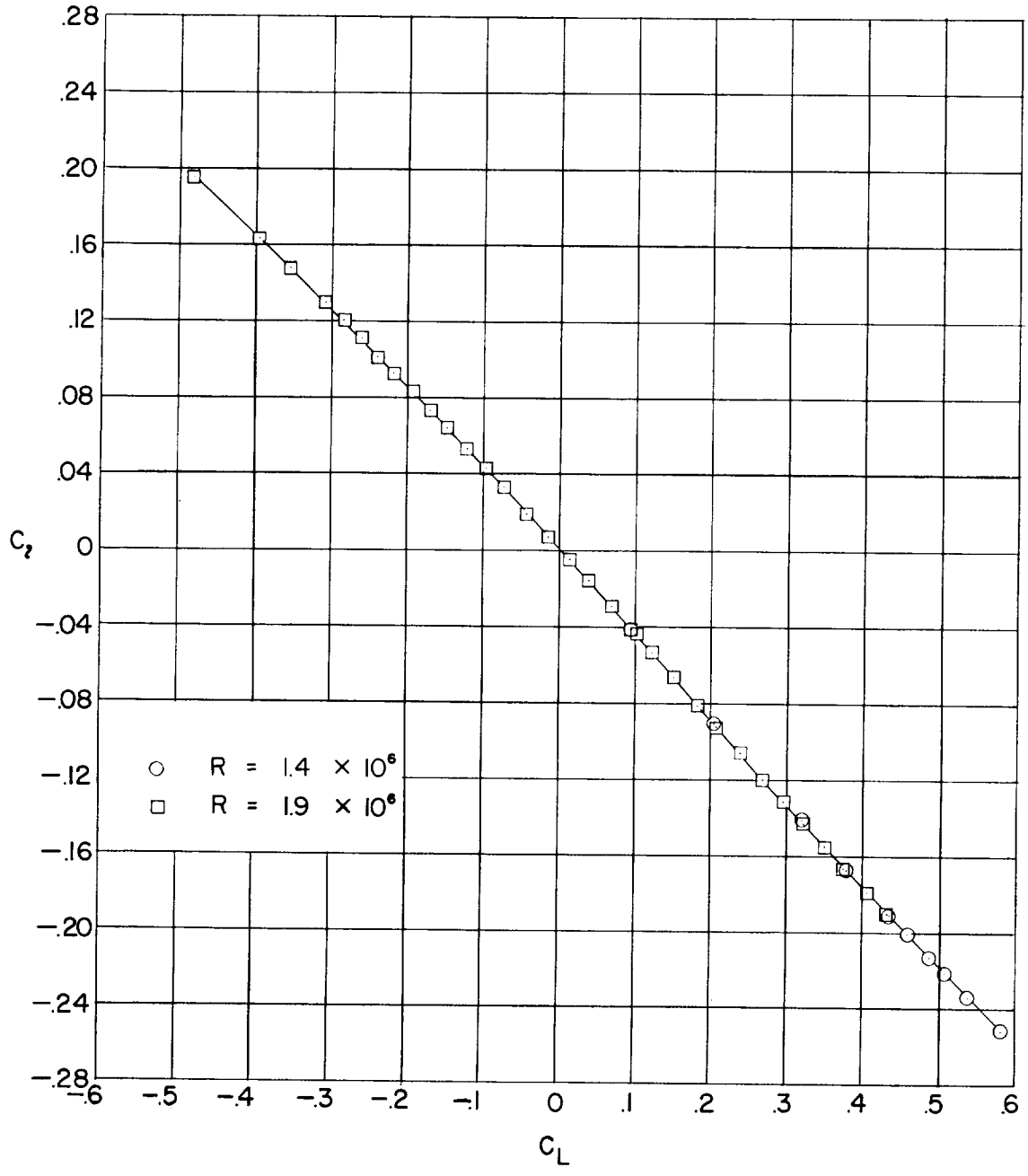

(c) Rolling-moment coefficient.

Figure 6.- Concluded.

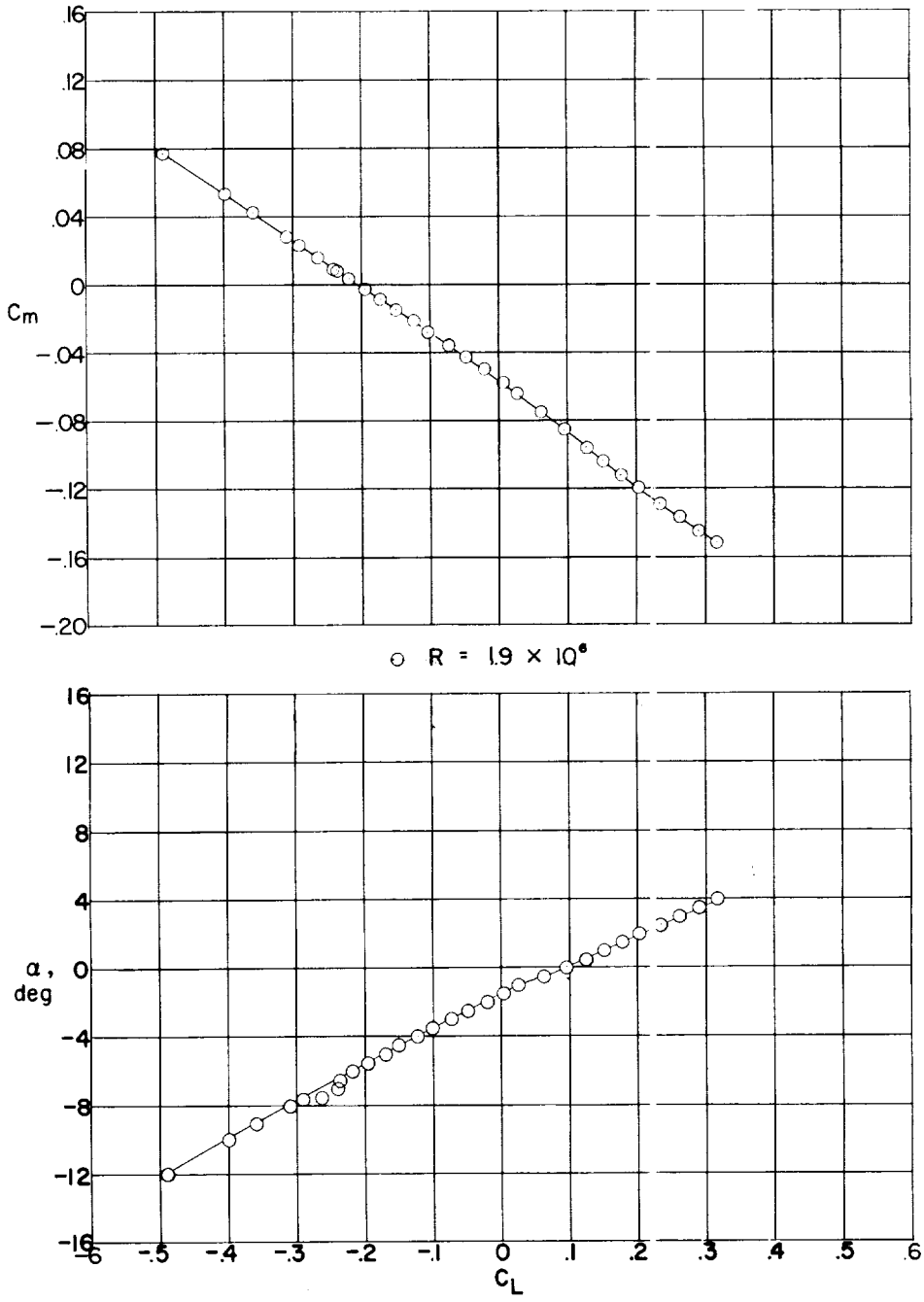

(a) Lift and pitching-moment coefficients.

Figure 7.- Aerodynamic characteristics of wing C with fixed transition. M = 1.61.

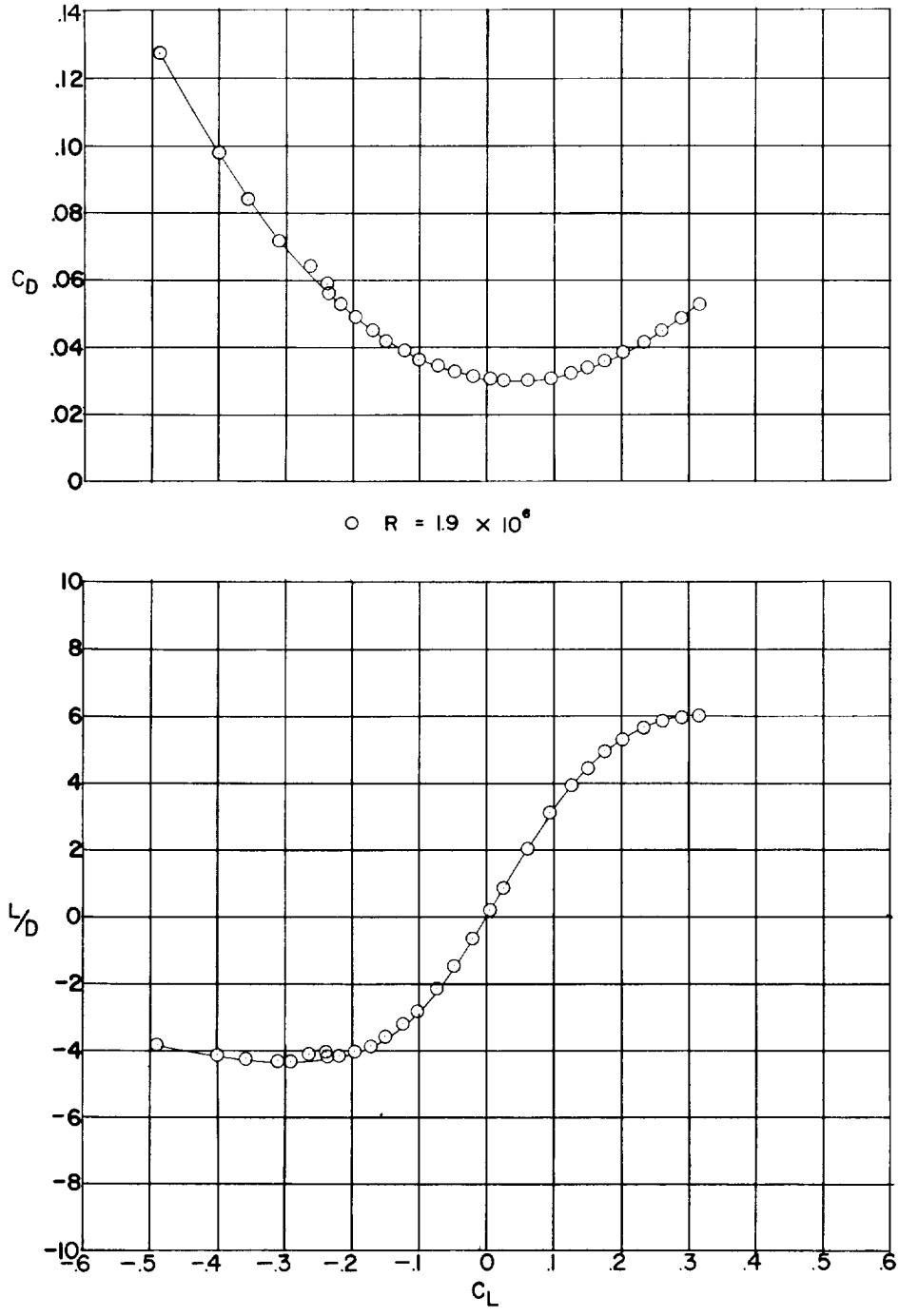

(b) Drag coefficient and lift-drag ratio.

Figure 7.- Continued.

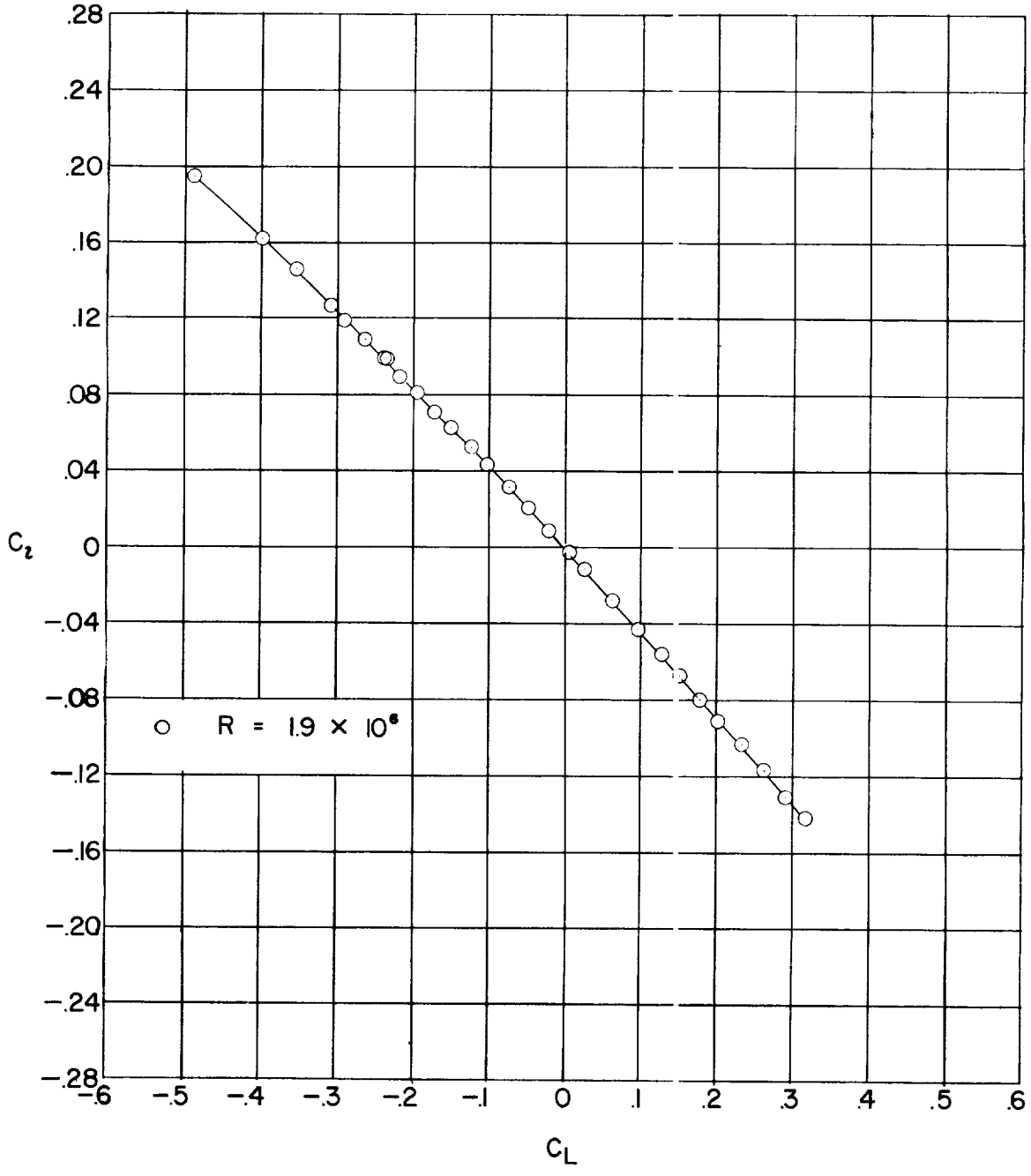

(c) Rolling-moment coefficient.

Figure 7.- Concluded.

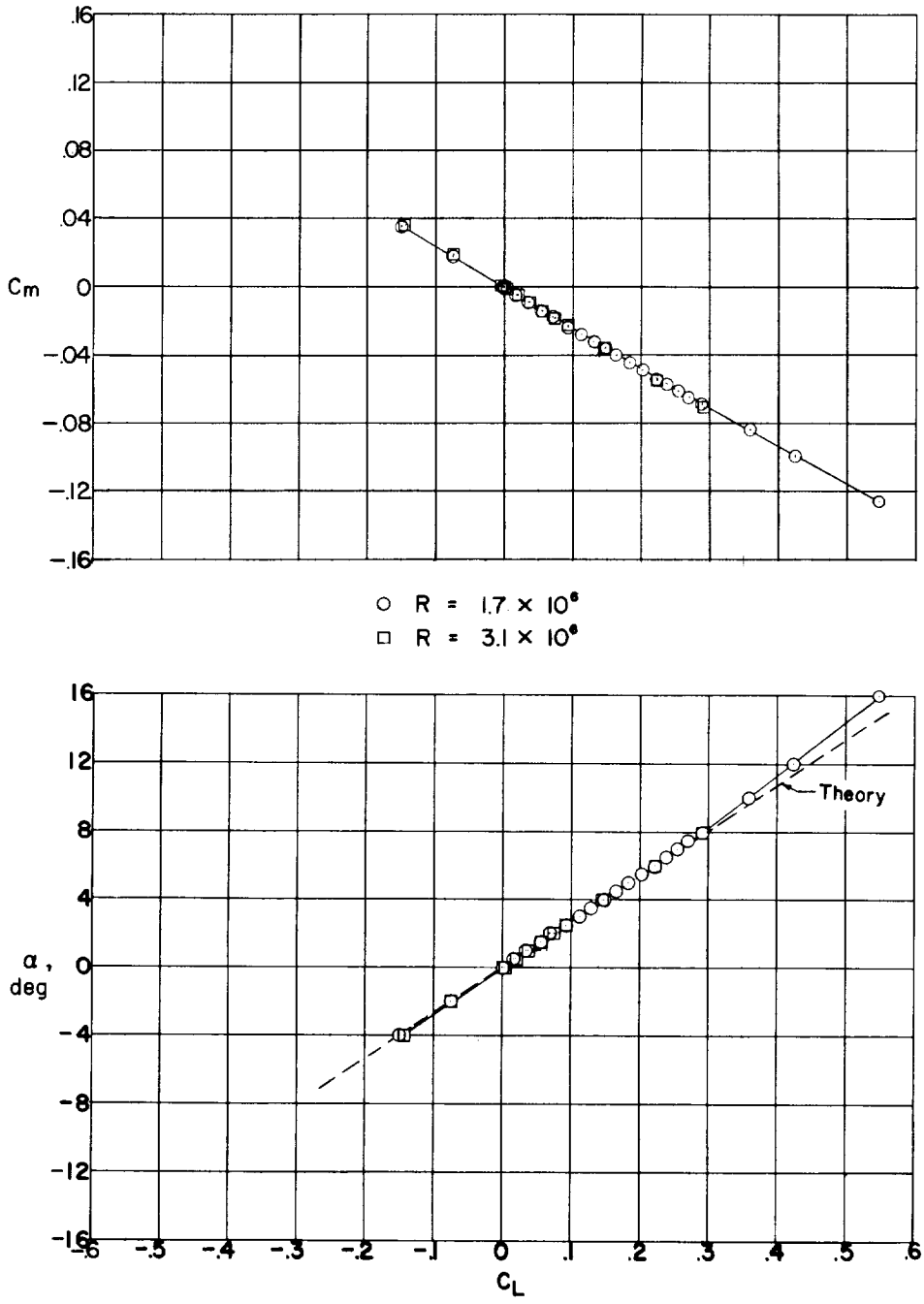

(a) Lift and pitching-moment coefficients.

Figure 8.- Aerodynamic characteristics of wing F with natural transition. M = 2.01.

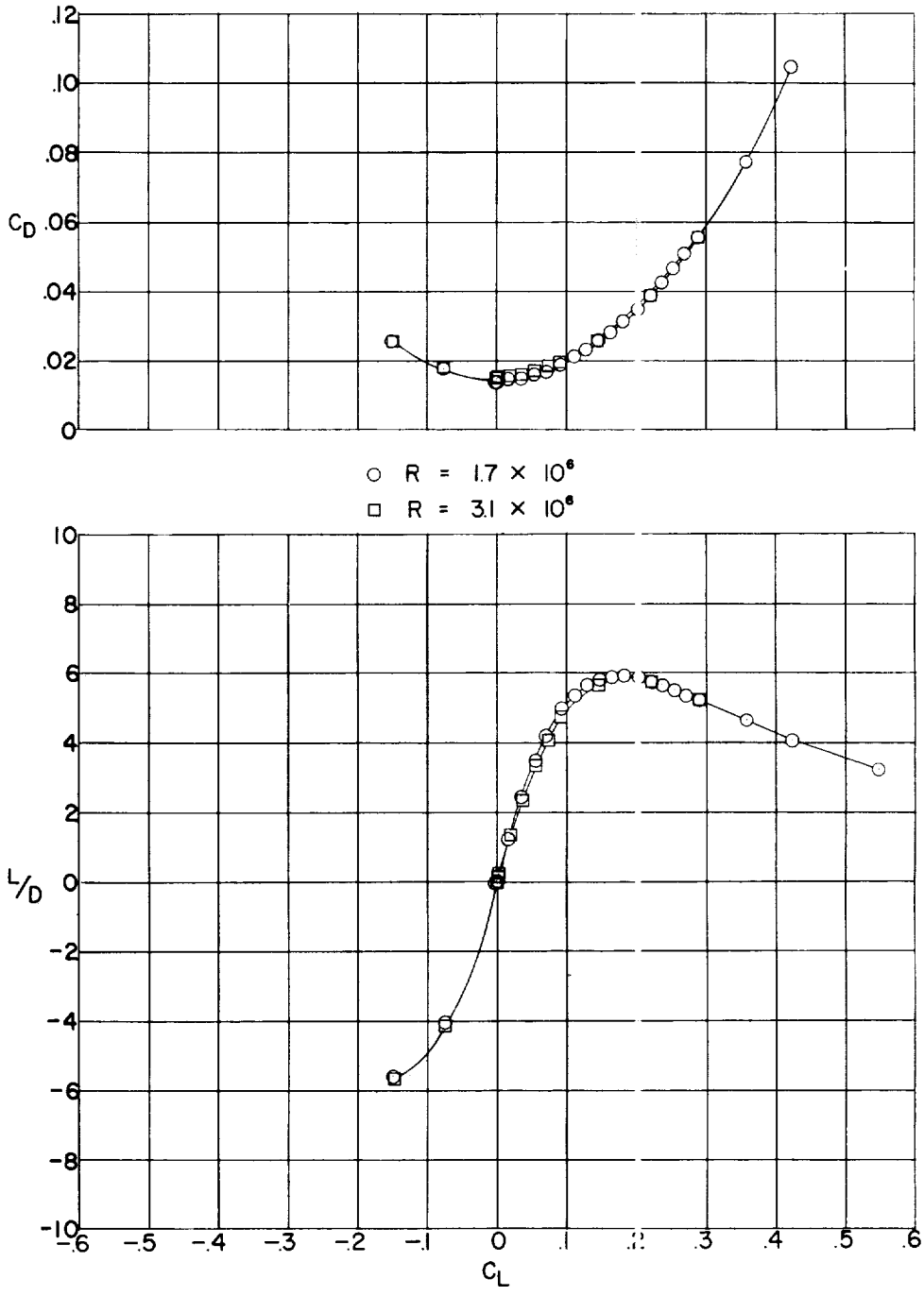

(b) Drag coefficient and lift-drag ratio.

Figure 8.- Continued.

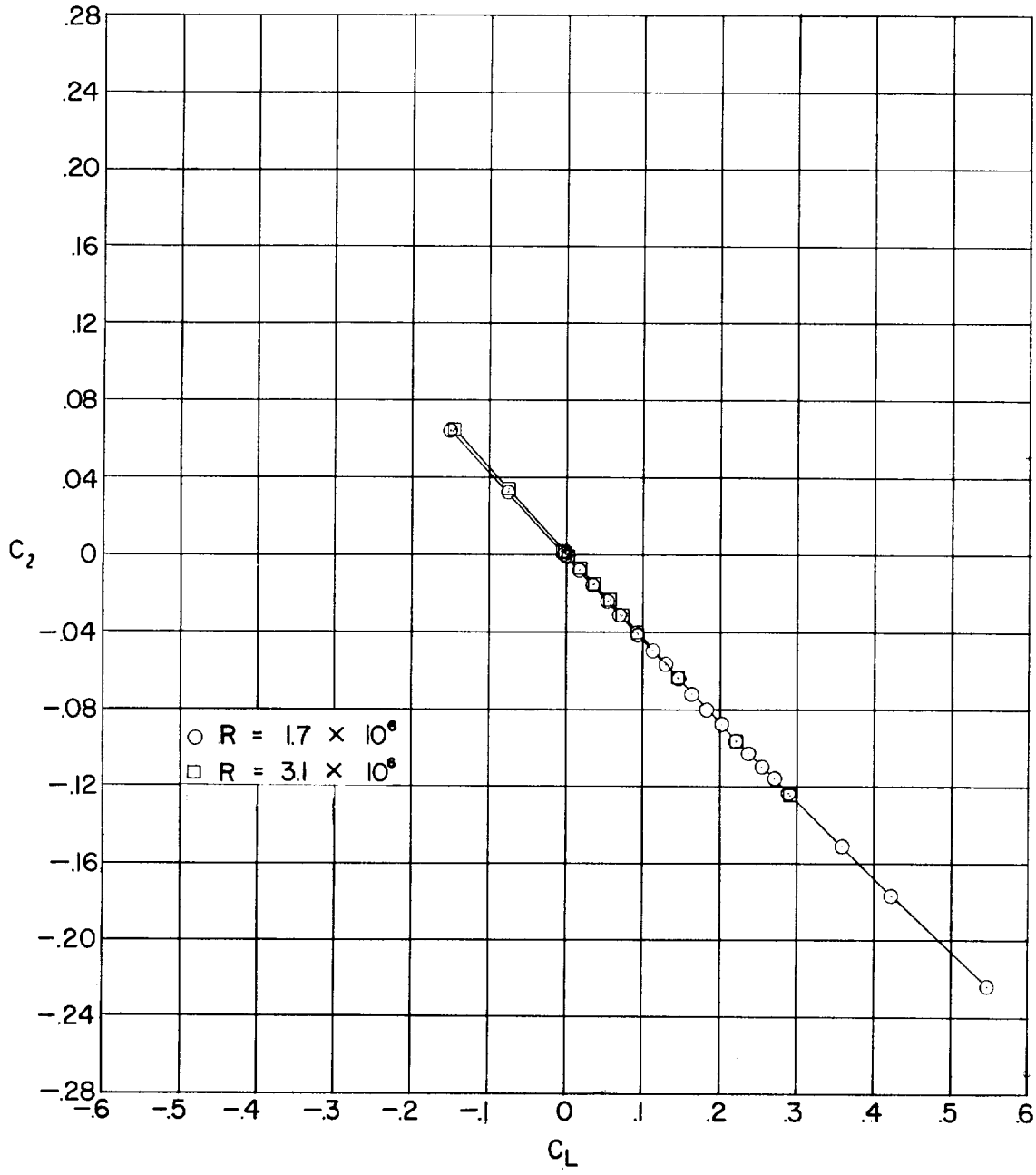

(c) Rolling-moment coefficient.

Figure 8.- Concluded.

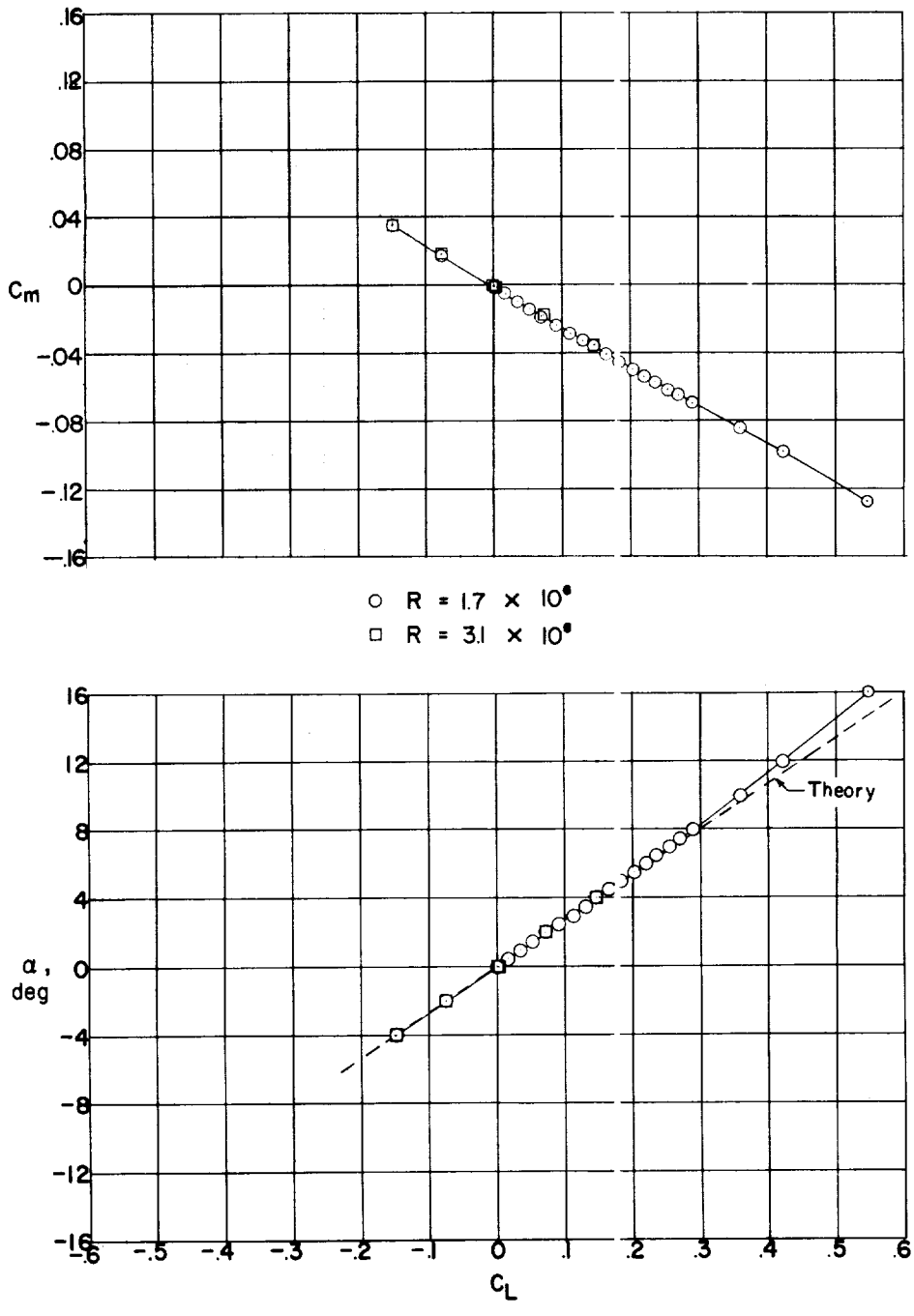

(a) Lift and pitching-moment coefficients.

Figure 9.- Aerodynamic characteristics of wing F with fixed transition. M = 2.01.

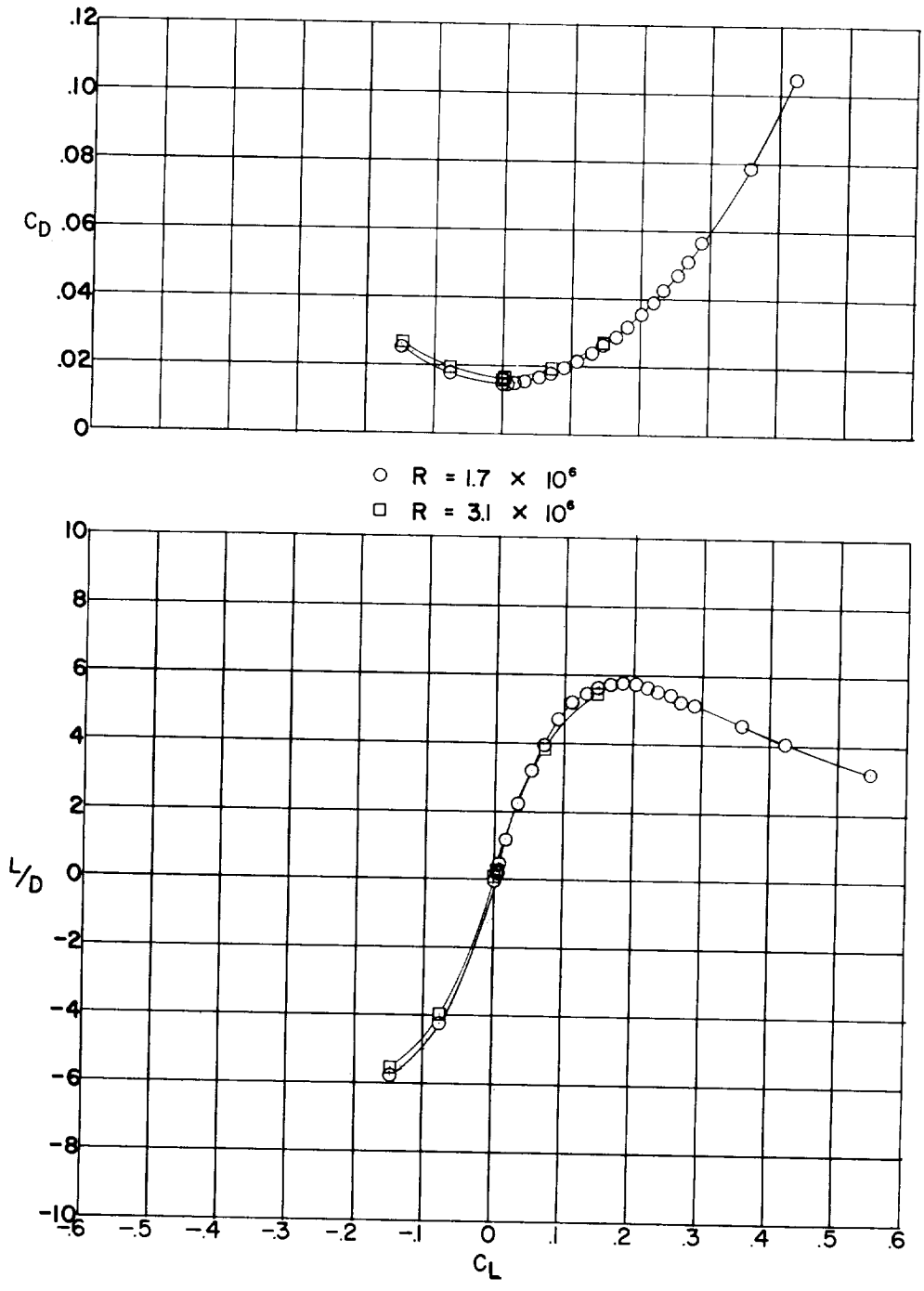

(b) Drag coefficient and lift-drag ratio.

Figure 9.- Continued.

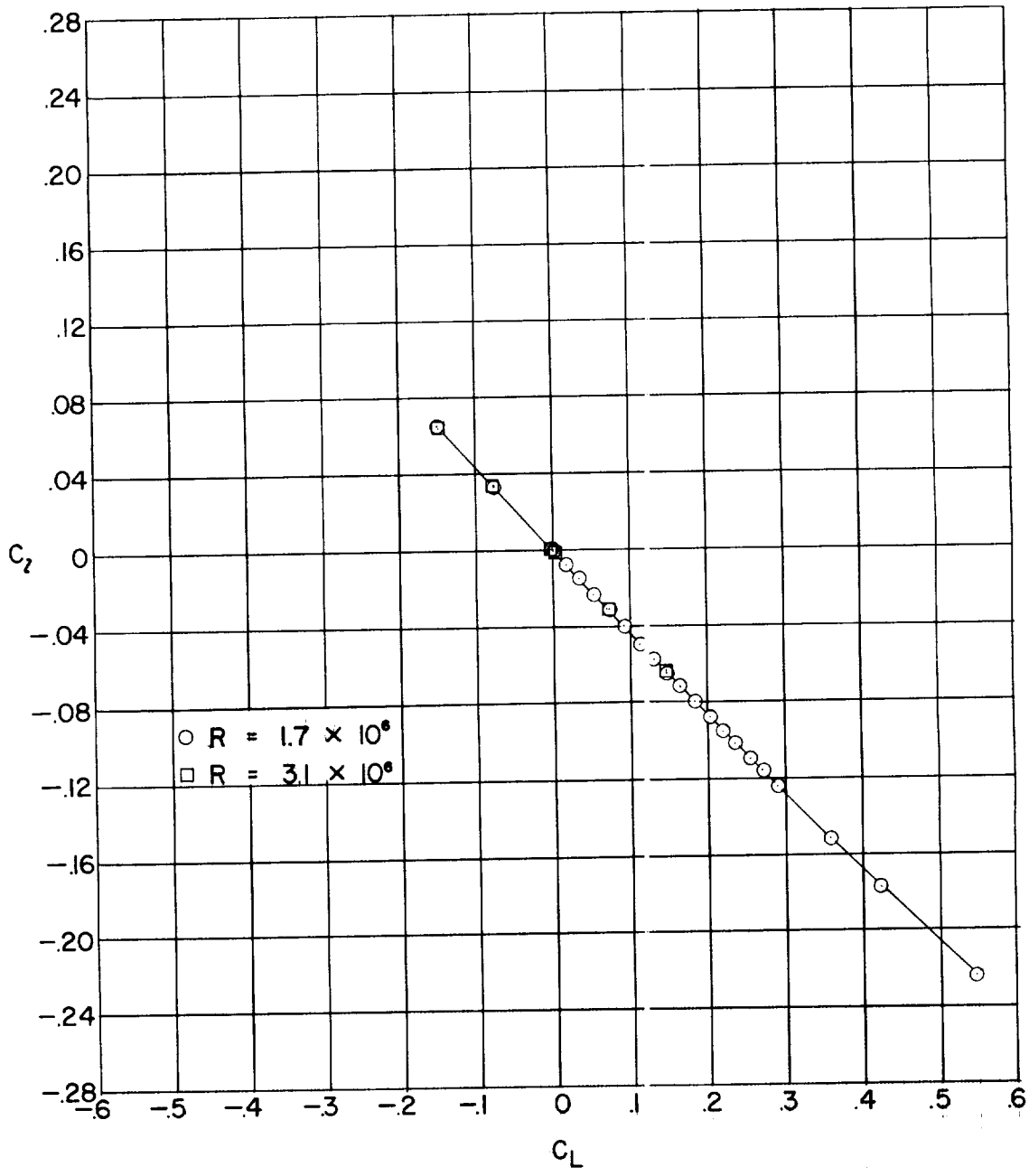

(c) Rolling-moment coefficient.

Figure 9.- Concluded.

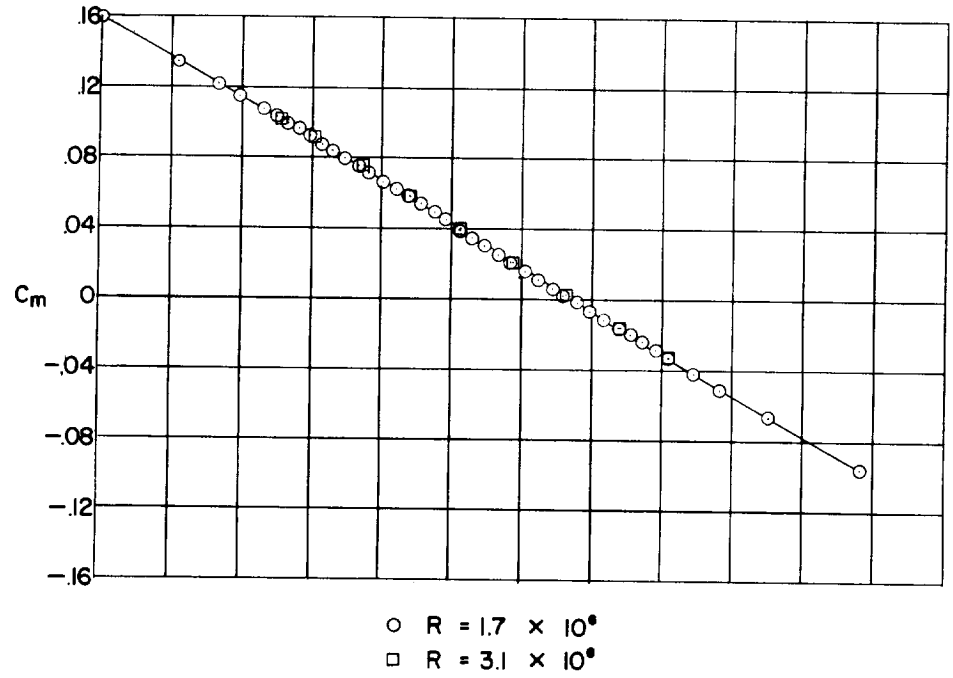

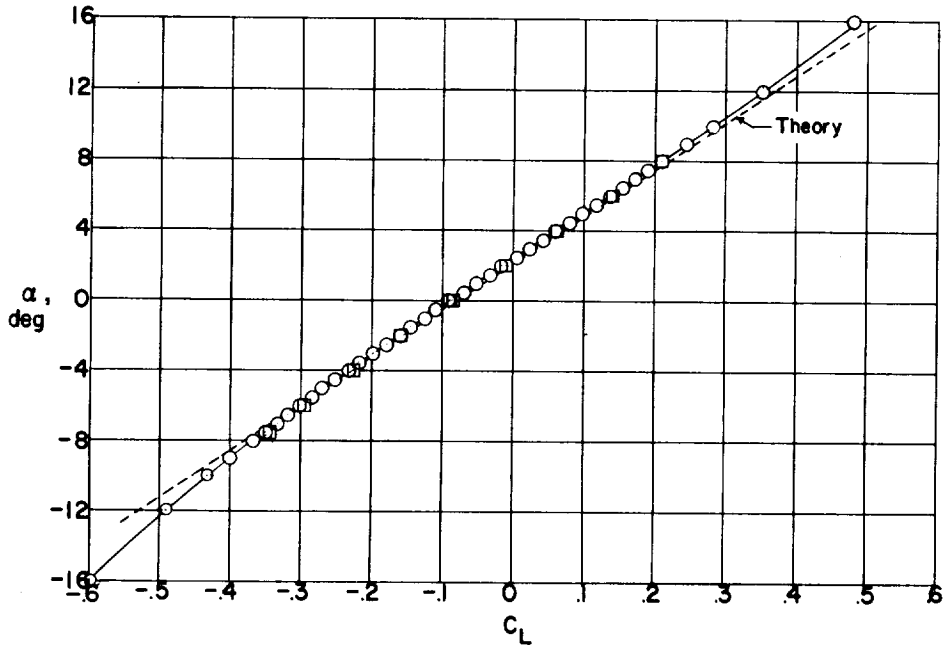

(a) Lift and pitching-moment coefficients.

Figure 10.- Aerodynamic characteristics of wing 1 with natural transition. M = 2.01.

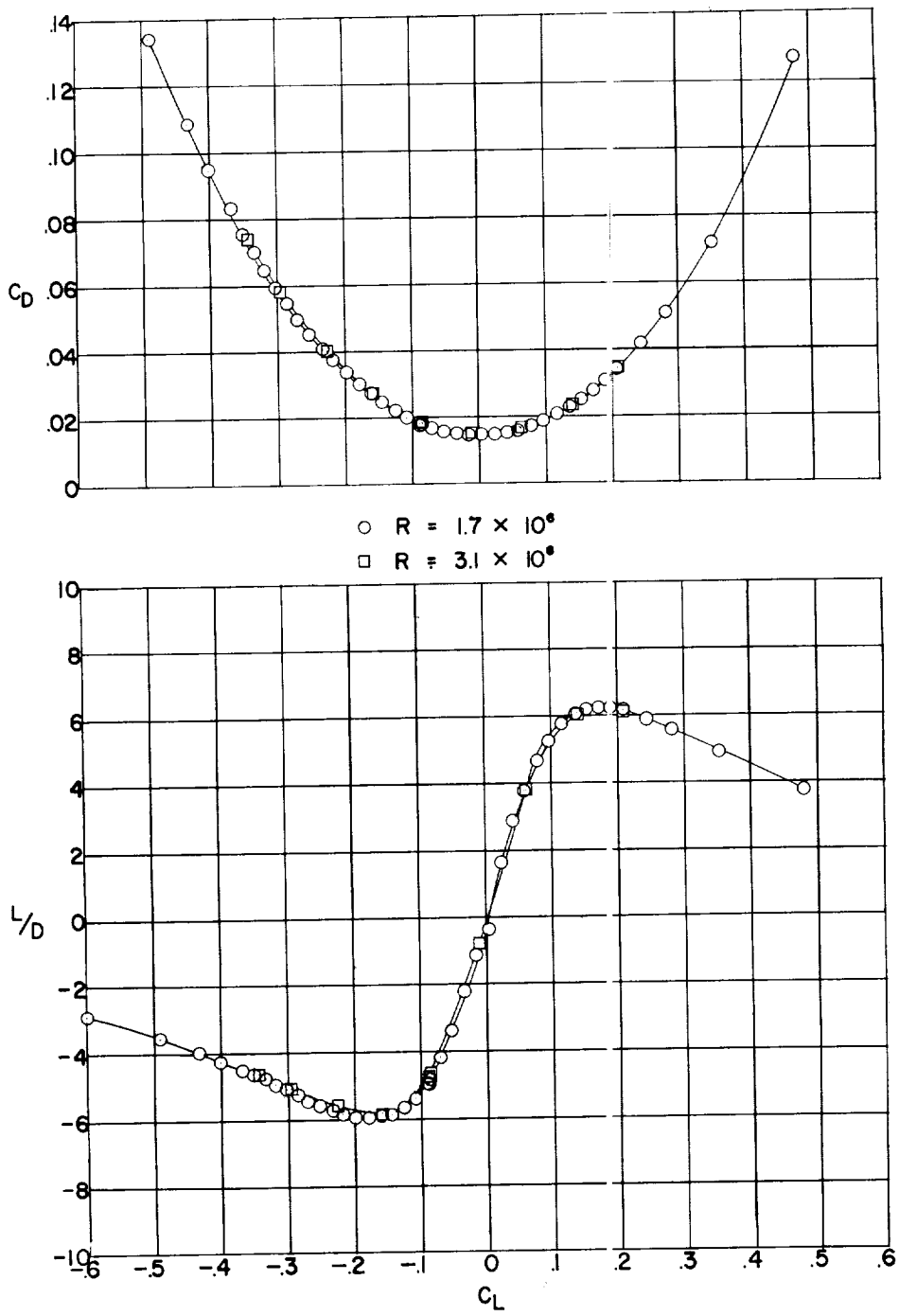

(b) Drag coefficient and lift-drag ratio.

Figure 10.- Continued.

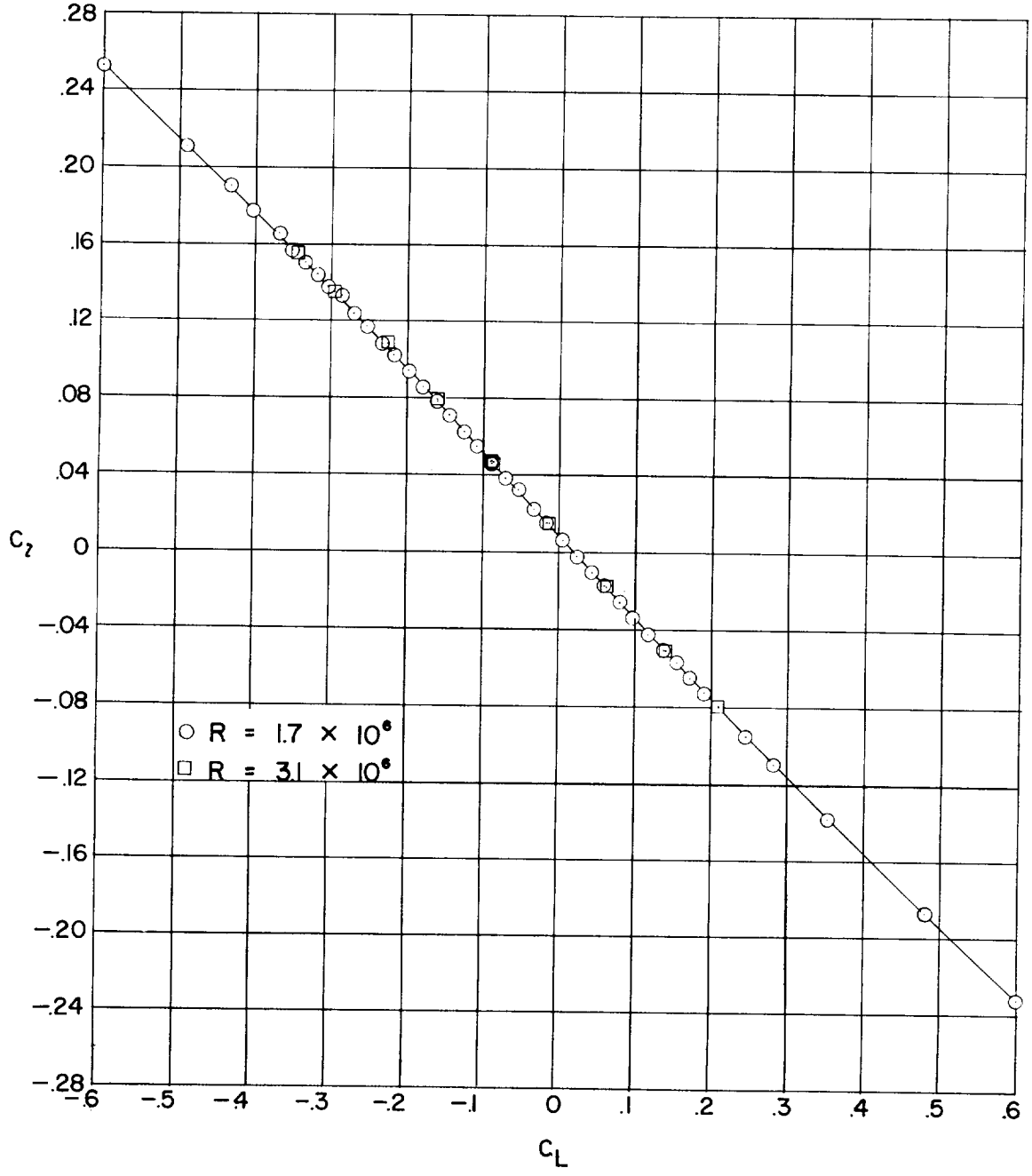

(c) Rolling-moment coefficient.

Figure 10.- Concluded.

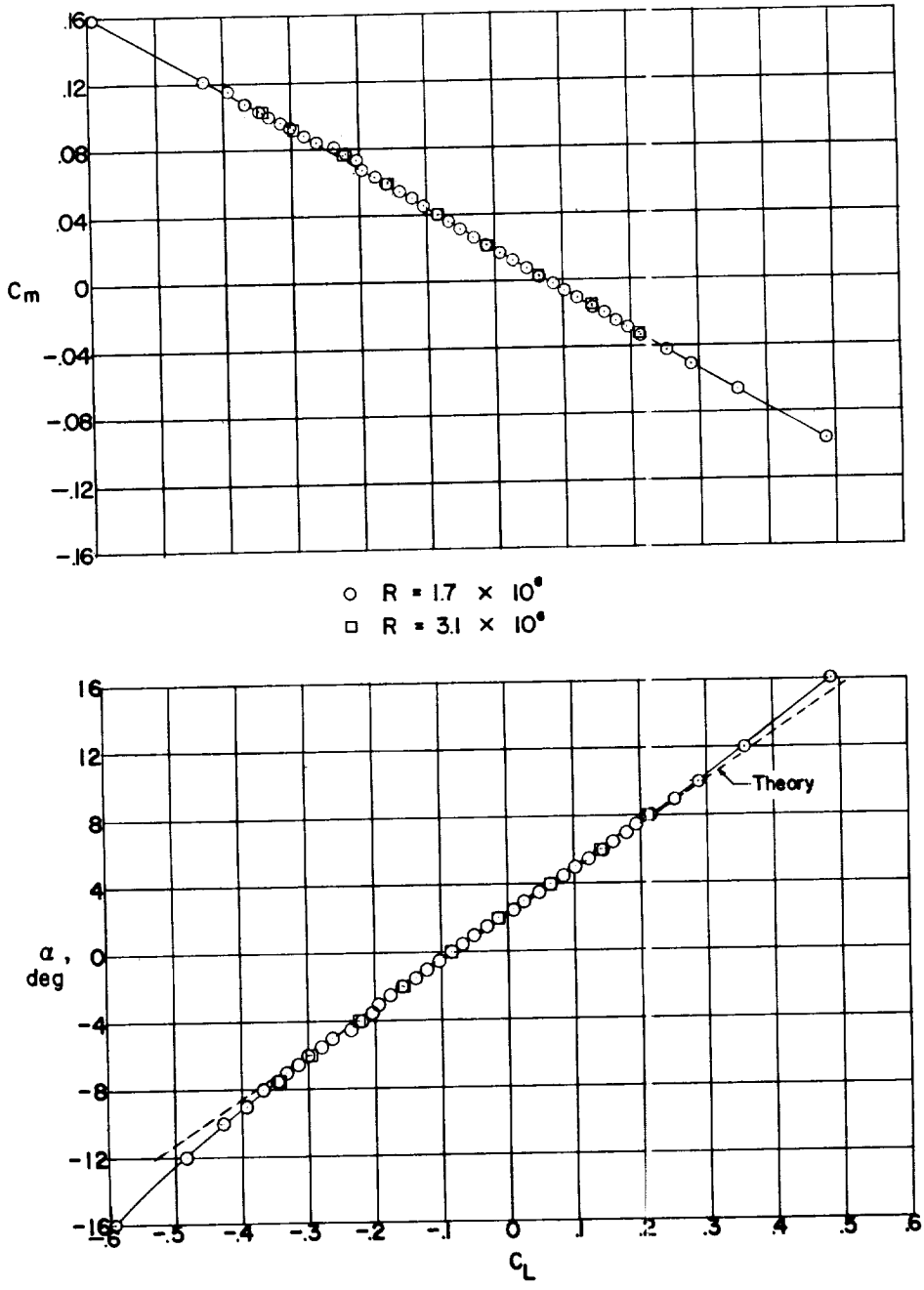

(a) Lift and pitching-moment coefficients.

Figure 11.- Aerodynamic characteristics of wing 1 with fixed transition. M = 2.01.

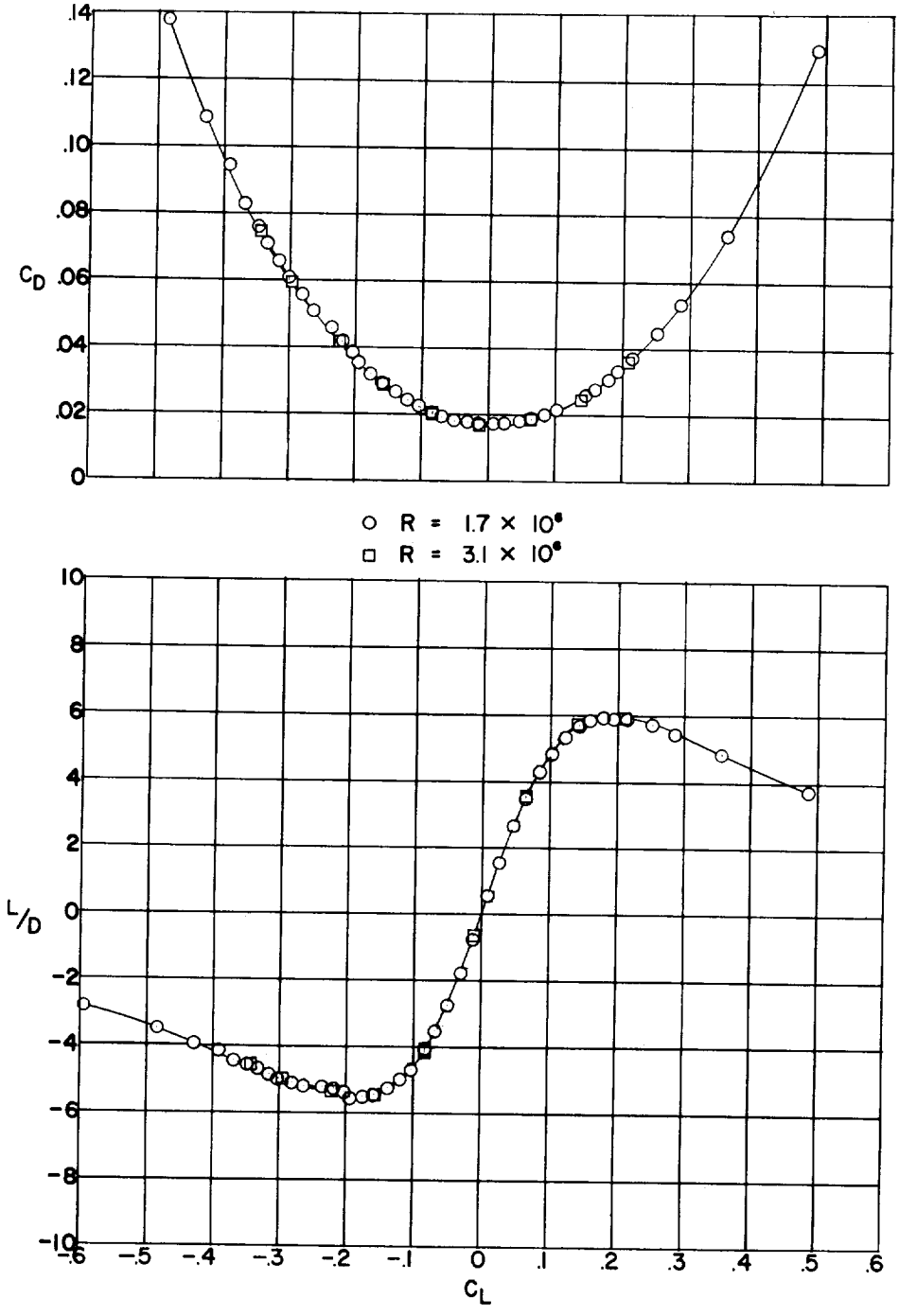

(b) Drag coefficient and lift-drag ratio.

Figure 11.- Continued.

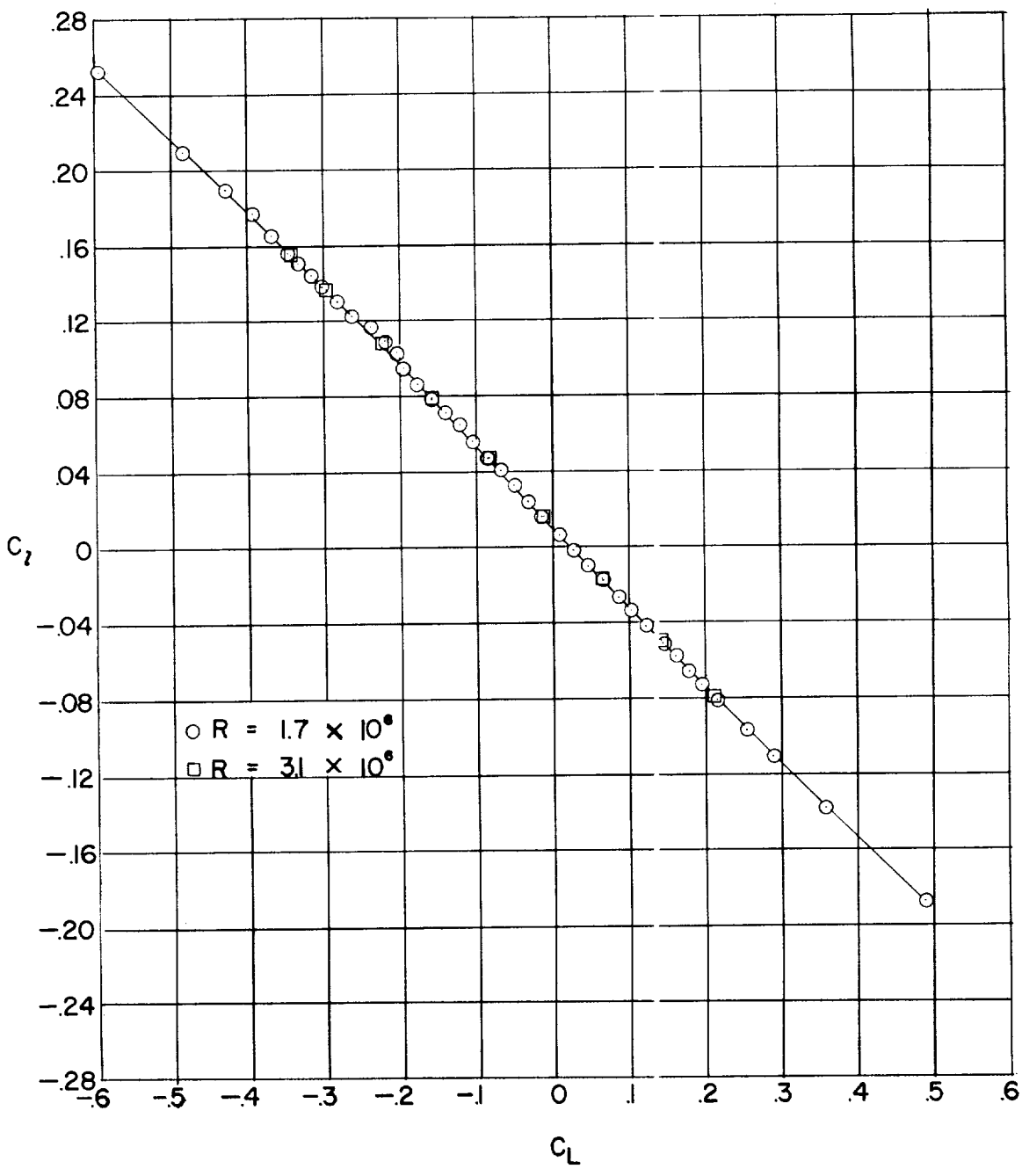

(c) Rolling-moment coefficient.

Figure 11.- Concluded.

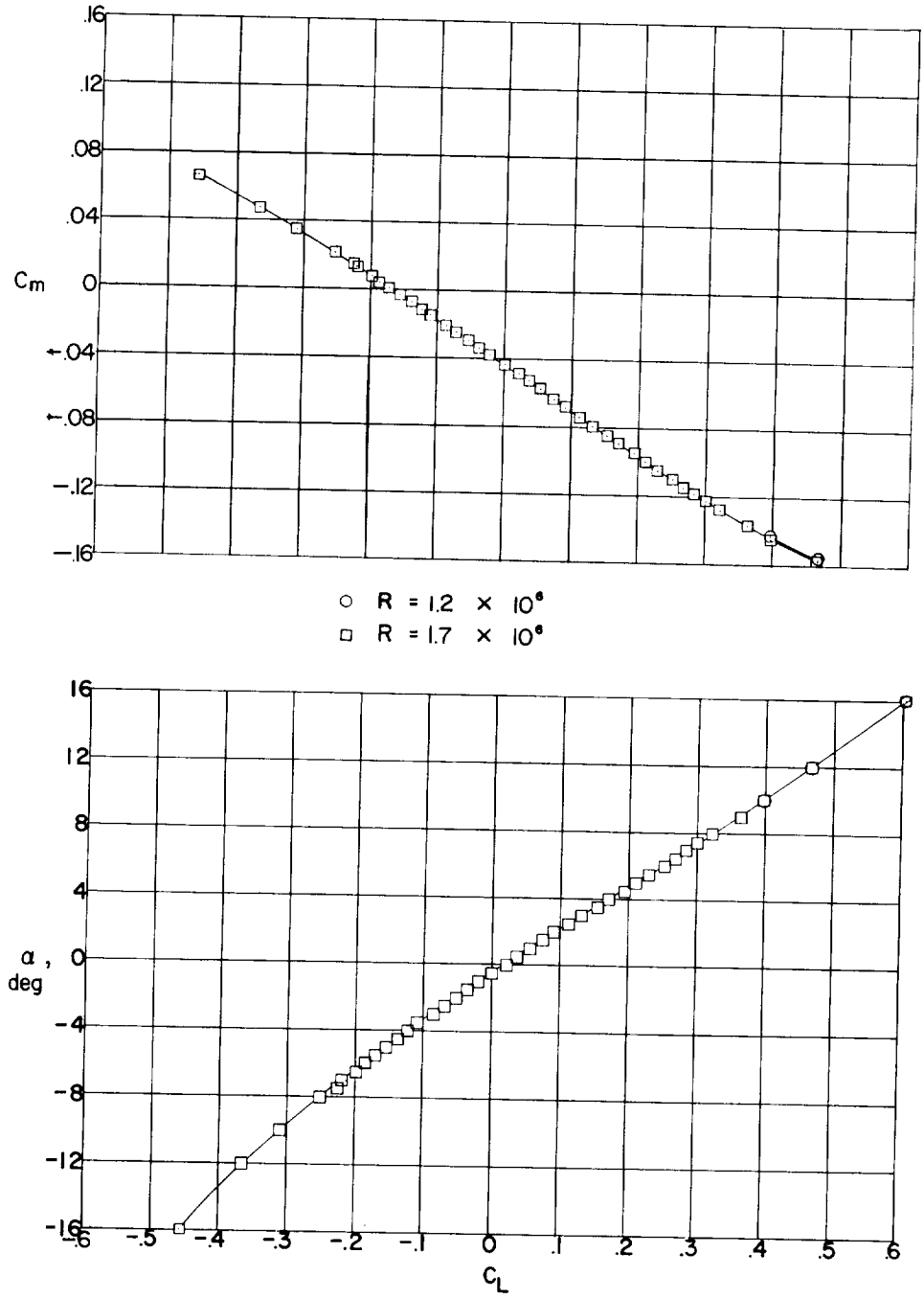

(a) Lift and pitching-moment coefficients.

Figure 12.- Aerodynamic characteristics of wing C with natural transition. M = 2.01.

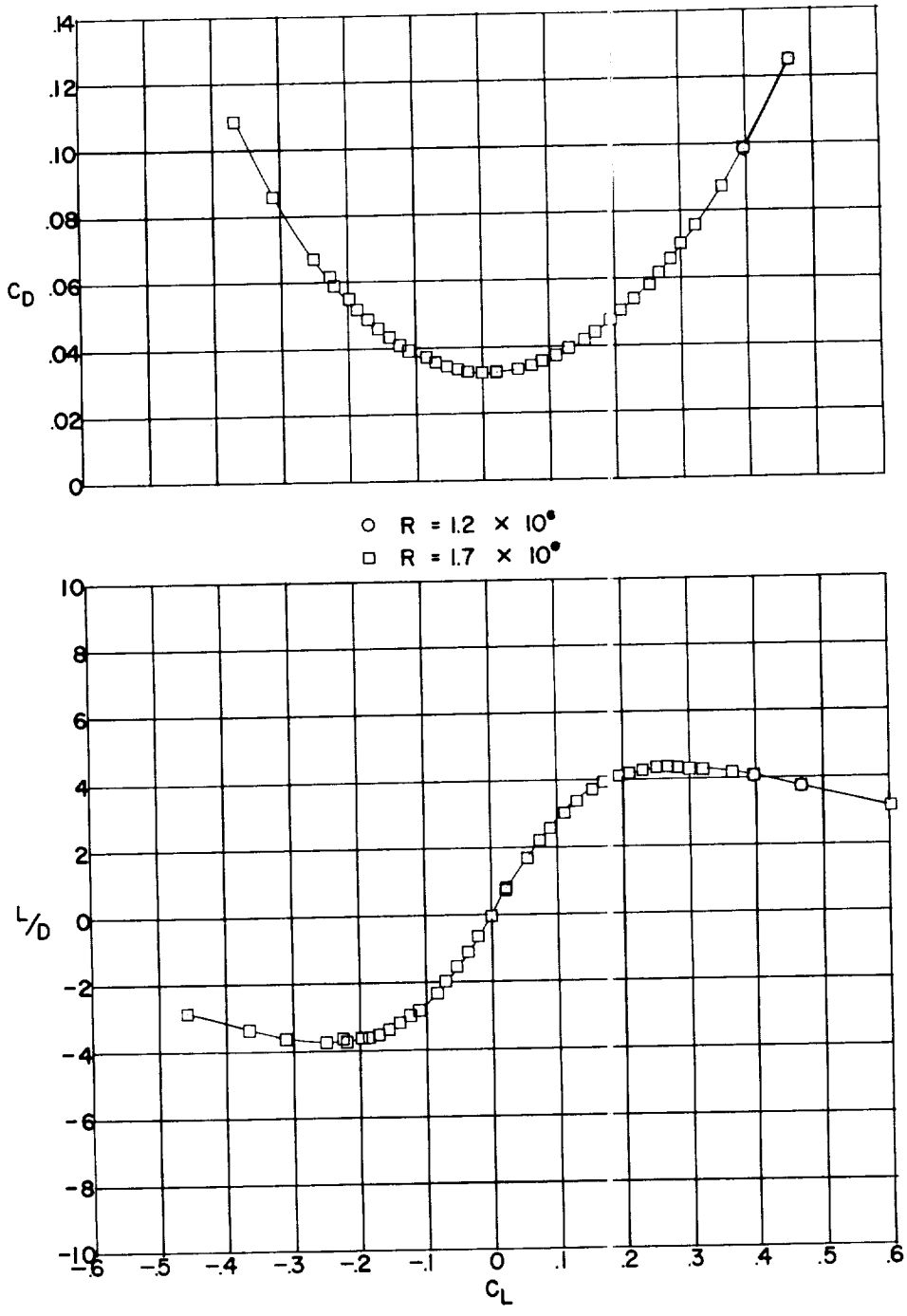

(b) Drag coefficient and lift-drag ratio.

Figure 12.- Continued.

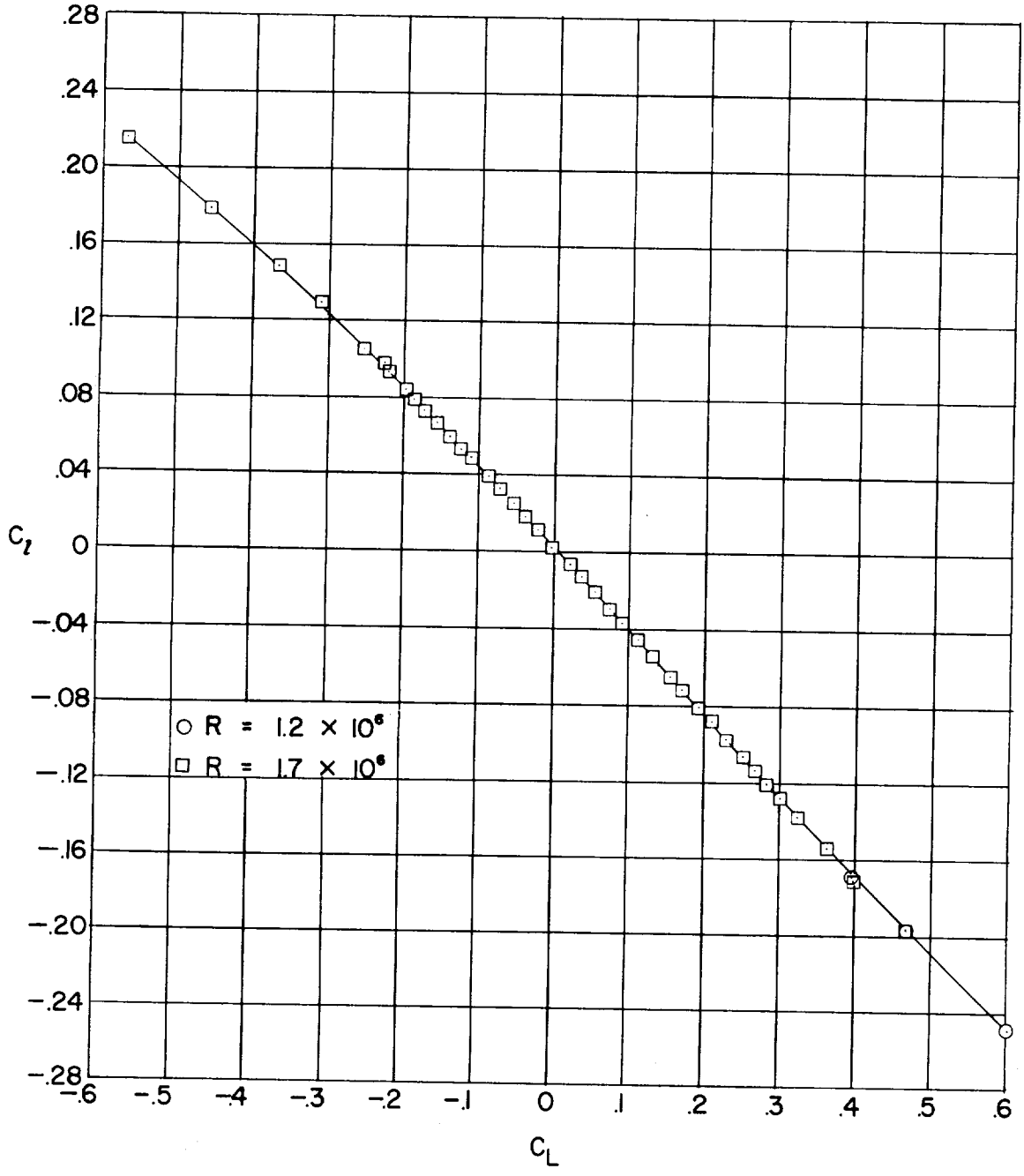

(c) Rolling-moment coefficient.

Figure 12.- Concluded.

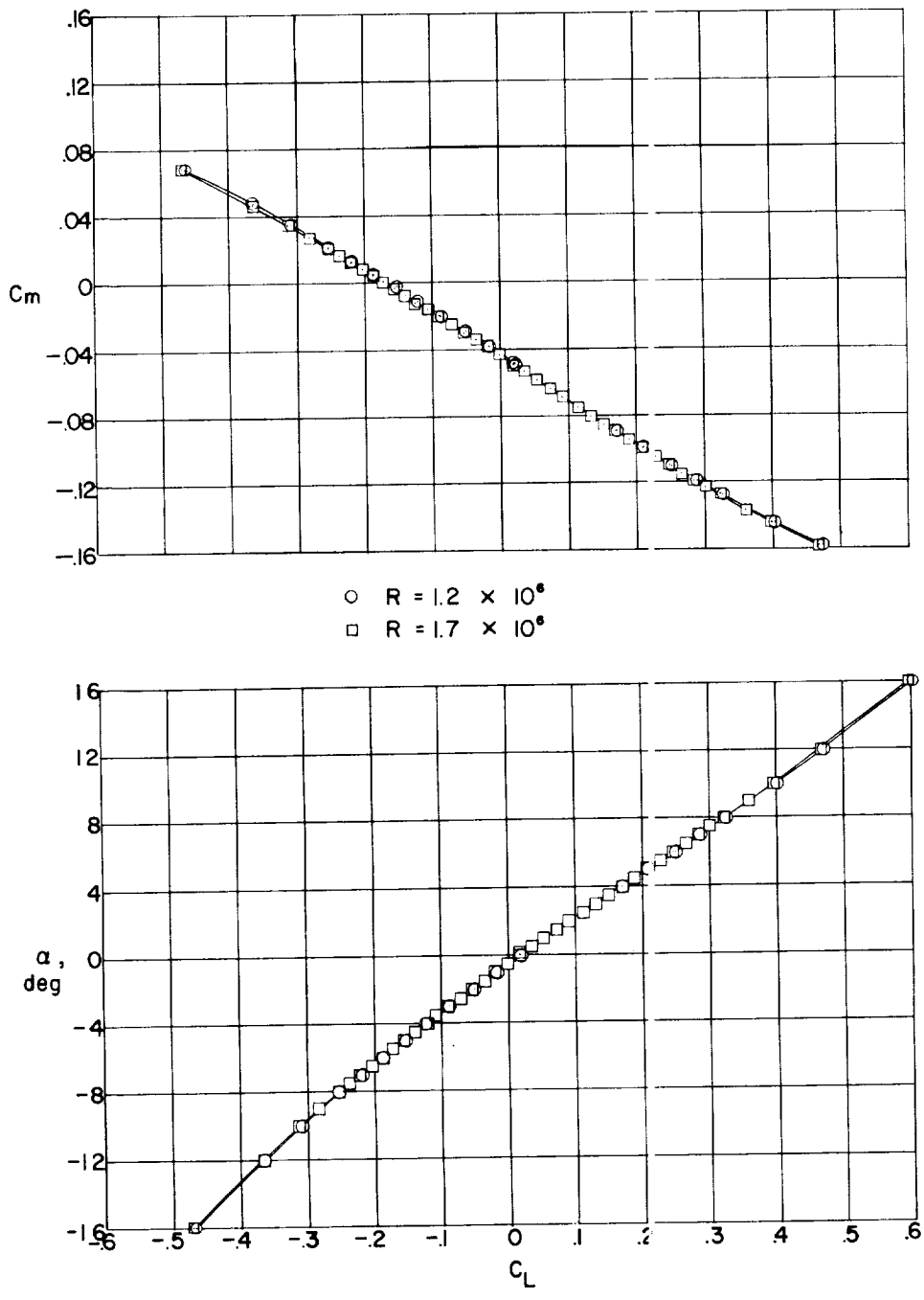

(a) Lift and pitching-moment coefficients.

Figure 13.- Aerodynamic characteristics of wing C with fixed transition. M = 2.01.

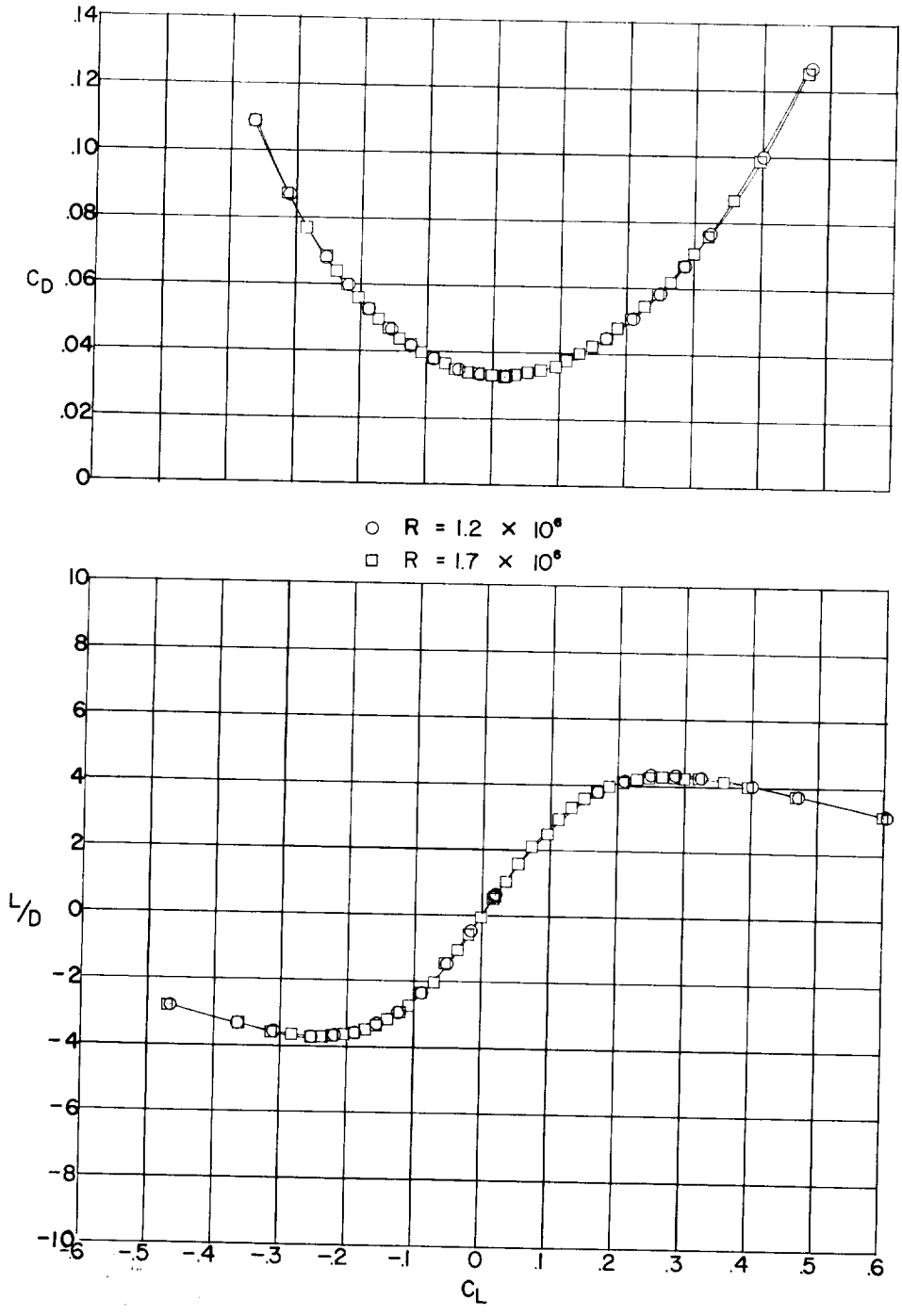

(b) Drag coefficient and lift-drag ratio.

Figure 13.- Continued.

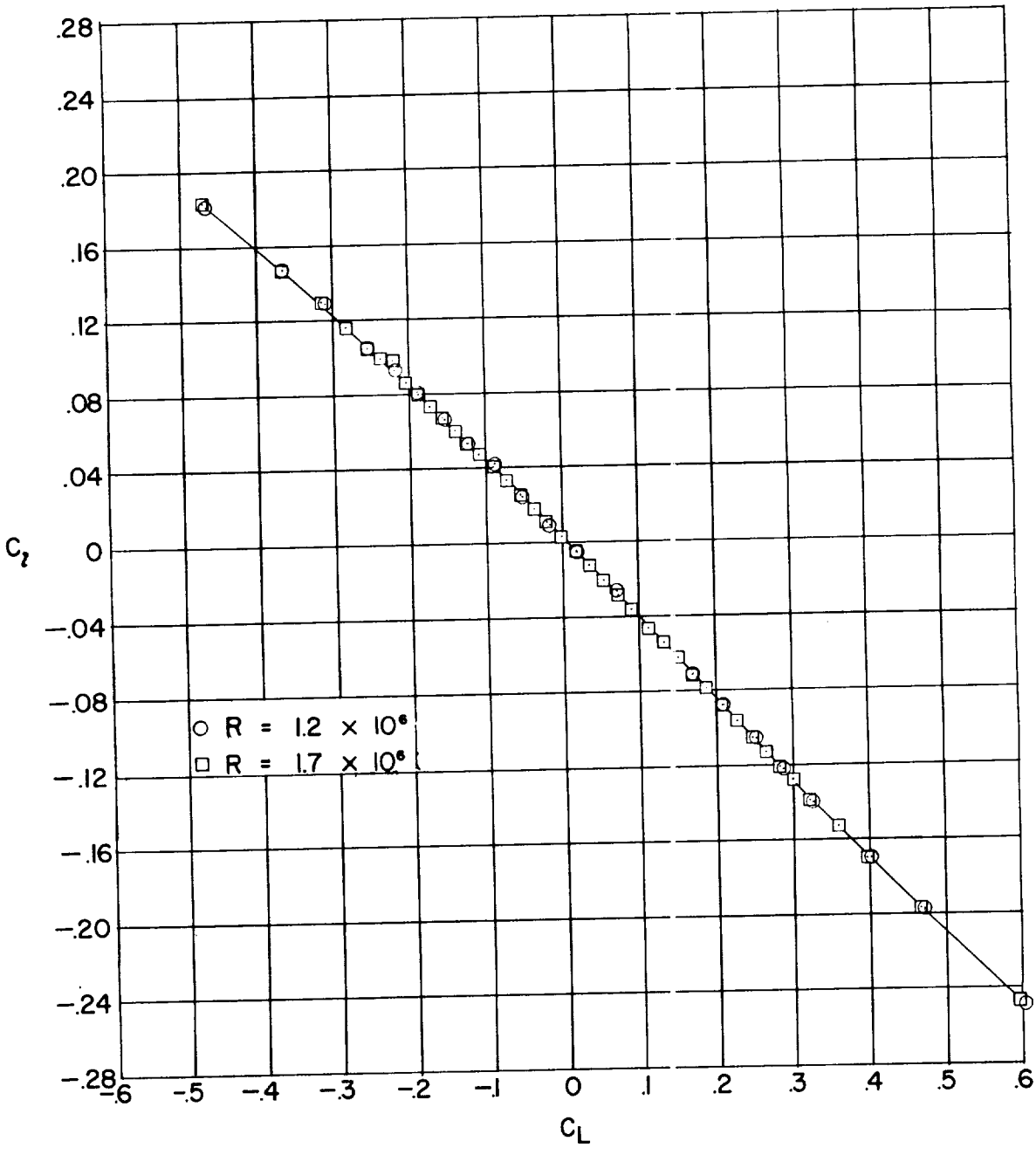

(c) Rolling-moment coefficient.

Figure 13.- Concluded.

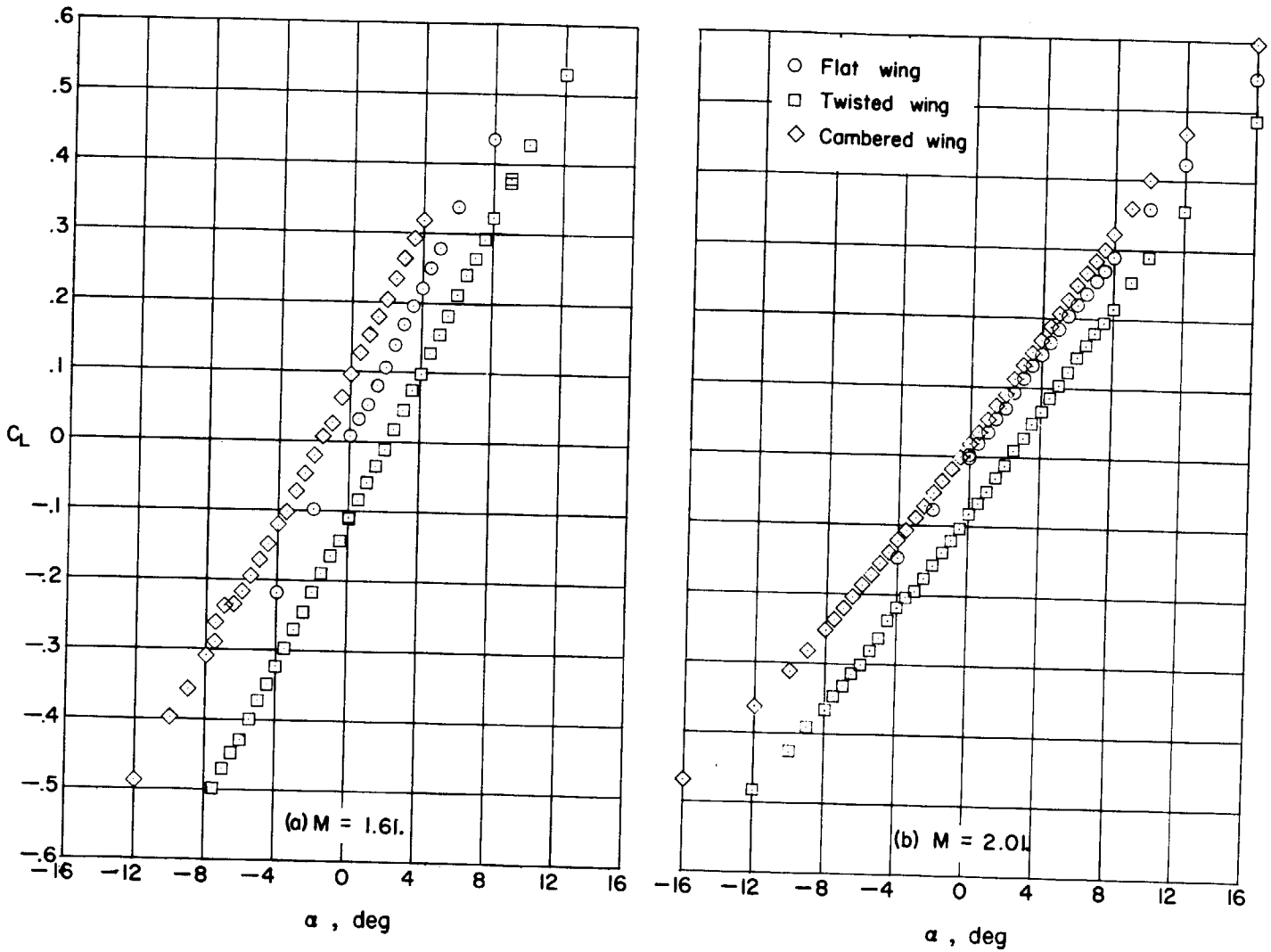

Figure 14.- Variation of C_L with α for the three wings. Fixed transition; $R \approx 1.8 \times 10^6$.

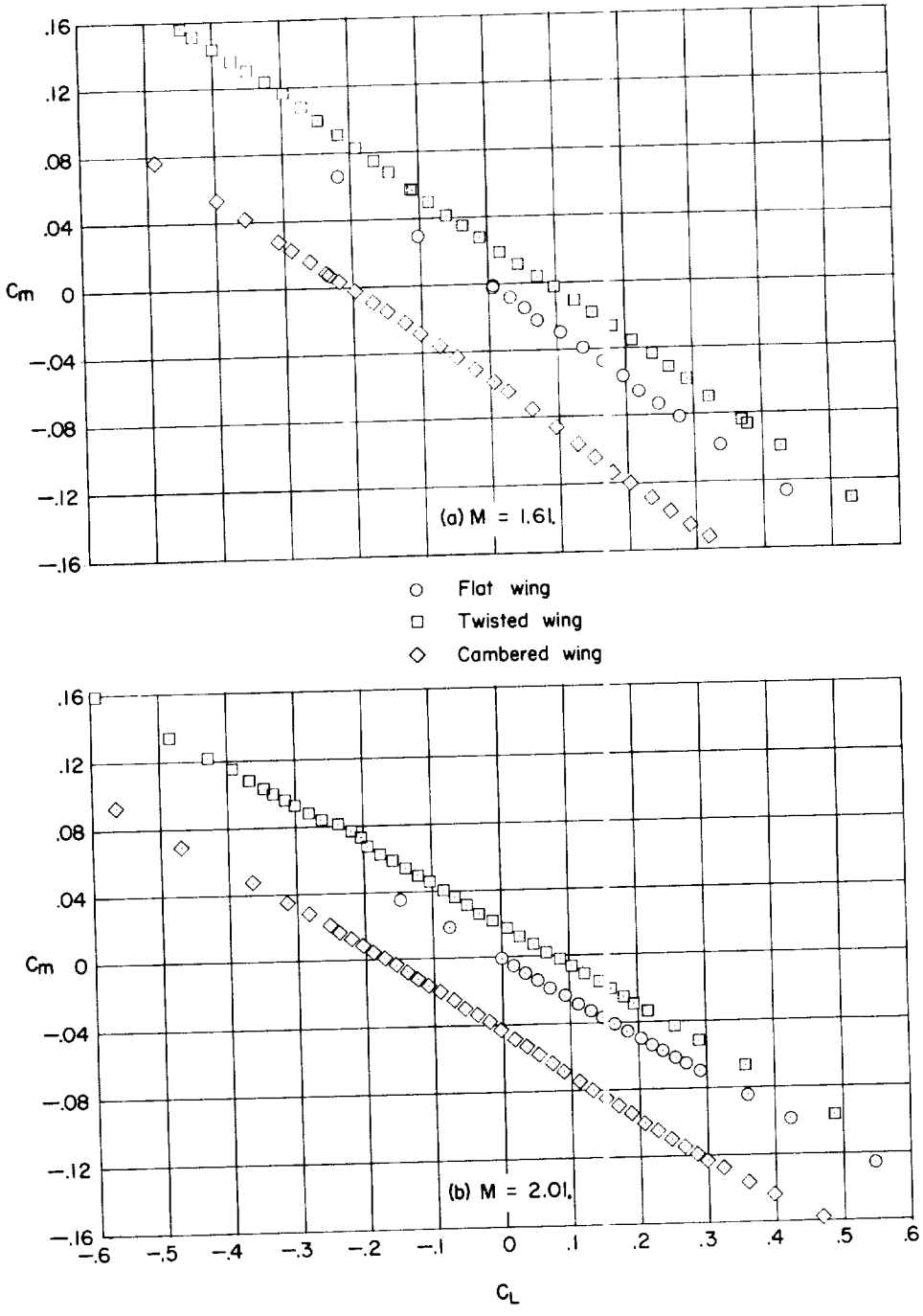

Figure 15.- Variation of C_m with C_L for the three wings. Fixed transition; $R \approx 1.3 \times 10^6$.

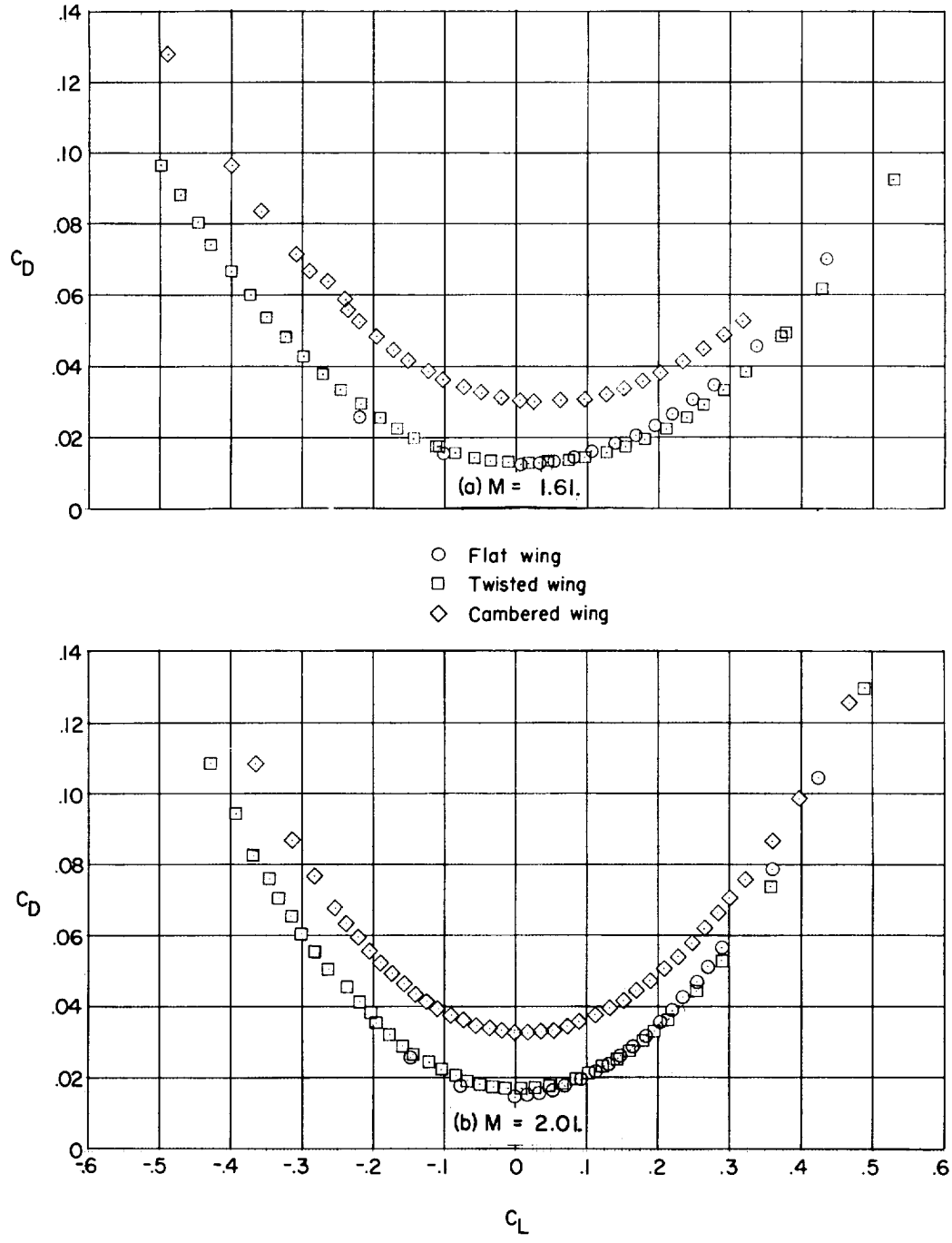

Figure 16.- Variation of C_D with C_L for the three wings. Fixed transition; $R \approx 1.8 \times 10^6$.

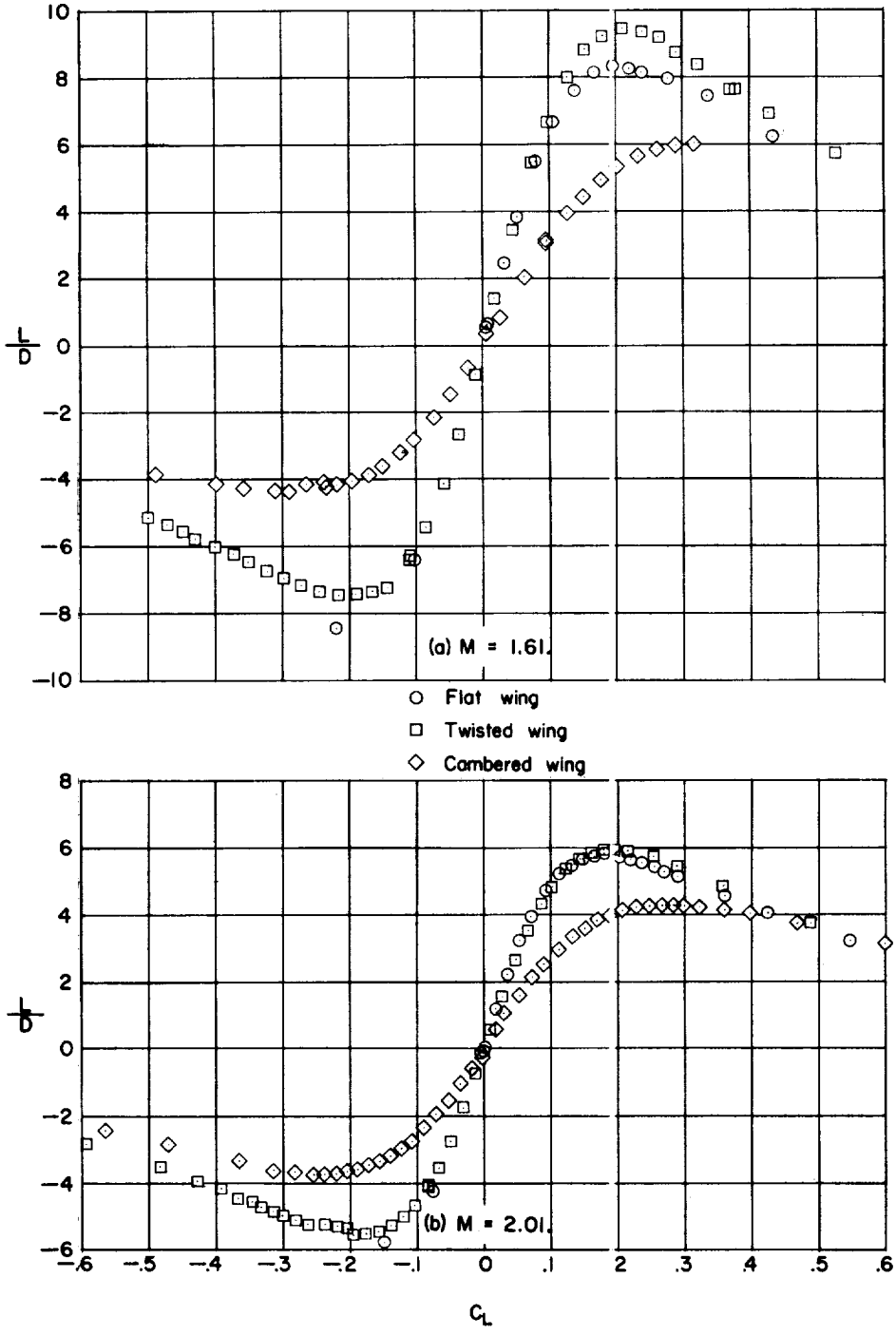

Figure 17.- Variation of L/D with C_L for the three wings. Fixed transition. $R \approx 1.8 \times 10^6$.

NASA - Langley Field, Va. L-1189